Structure/function studies on the bacterial carbohydrate transporters, enzymes II, of the phosphoenolpyruvate-dependent phosphotransferase system

Robillard, G.T.; Broos, J.

Published in:
Biochimica et Biophysica Acta-Reviews on Biomembranes

DOI:
10.1016/S0304-4157(99)00002-7

Publication date:
1999

ELSEVIER

Biochimica et Biophysica Acta 1422 (1999) 73–104

BIOCHIMICA ET BIOPHYSICA ACTA
BBA

www.elsevier.com/locate/bba

Structure/function studies on the bacterial carbohydrate transporters, enzymes II, of the phosphoenolpyruvate-dependent phosphotransferase system[1, 2]

G.T. Robillard *, J. Broos

The University of Groningen, Groningen Biomolecular Sciences and Biotechnology Institute, Nienborgh 4, 9747 AG Groningen, The Netherlands

Received 15 September 1998; received in revised form 27 January 1999; accepted 1 February 1999

Keywords: Fluorescence; Calorimetry; Nuclear Magnetic Resonance; X-ray structures; Facilitated diffusion; Non-vectorial phosphorylation

Contents

Abbreviations: PTS, phosphotransferase system; TMH, transmembrane helix; PEG, polyethylene glycol; NEM, *N*-ethylmaleimide; PEP, phosphoenolpyruvate; HPr, histidine-containing protein of the PTS; EII, enzyme II of the PTS; EI, enzyme I of the PTS; RSO, right-side-out; ISO, inside-out; GuHCl, guanidine hydrochloride; CD, circular dichroism; DSC, differential scanning calorimetry; ITC, isothermal titration calorimetry; DMPC, dimyrostoyl phosphatidylcholine; NOE, nuclear Overhauser effect; NOESY, nuclear Overhauser effect spectroscopy; HMQC, heteronuclear multiple quantum correlation; HSQC, heteronuclear single quantum correlation; GK, glycerol kinase; GGBP, galactose–glucose binding protein; PTPase, protein tyrosine phosphatase; ABP, arabinose binding protein; FTIR, Fourier transform infrared; PDB, protein data base

* Corresponding author. Fax: +31-50-363-4429; E-mail: g.t.robillard@chem.rug.nl

[1] Nomenclature: When referring to a domain in a multidomain EII we use the terminology 'A domain', 'B domain' etc. When referring to a domain of EII which has been subcloned and expressed as a separate protein we refer to it as, for example, 'IIA^{mtl}', 'IIB^{glc}', etc.

[2] Notation: heterodimers formed by mixing or co-expressing two proteins are denoted protein 1/protein 2 (i.e., wild-type/H554A or C384S/H195A). Double mutants are denoted as mutation1:mutation2 (i.e., C384S:H195A).

PII: S0304-4157(99)00002-7

1. Introduction

The phosphoenolpyruvate-dependent carbohydrate transport system is responsible for the transport of a variety of carbohydrates in prokaryotes at the expense of phosphoenolpyruvate (PEP). It consists of the general phosphotransferase system (PTS) proteins, Enzyme I and HPr, which are usually situated in the cytoplasm, carbohydrate-specific transporters, which are situated in the cytoplasmic membrane and additional carbohydrate-specific proteins, which can be either cytoplasmic or membrane-bound (see Fig. 1). Comprehensive reviews on the phosphoenolpyruvate-dependent phosphotransferase system have been published in recent years [1–4]. The purpose of the present treatment will be to examine the current state of our understanding of the structure and mechanism of action of the carbohydrate-specific components, the family of PTS Enzymes II (EII). This information has been collected from biophysical and kinetic investigations which have focused mainly on EII^{mtl} and to a lesser extent on EII^{glc} and EII^{man} all from *E. coli*. EIIs catalyze the following four reactions:

- transport of PTS-specific carbohydrates, hexoses and hexitols, from the periplasmic to the cytoplasmic space coupled with their phosphorylation (vectorial phosphorylation);
- phosphorylation of these carbohydrates from the cytoplasmic side of the membrane (non-vectorial phosphorylation);
- exchange, a reaction in which carbohydrate-phosphate, the product of the normal forward reaction, acts as a phosphoryl donor for another carbohydrate molecule, the phosphoryl group being transferred via EII;
- facilitated diffusion of the carbohydrate over the cytoplasmic membrane.

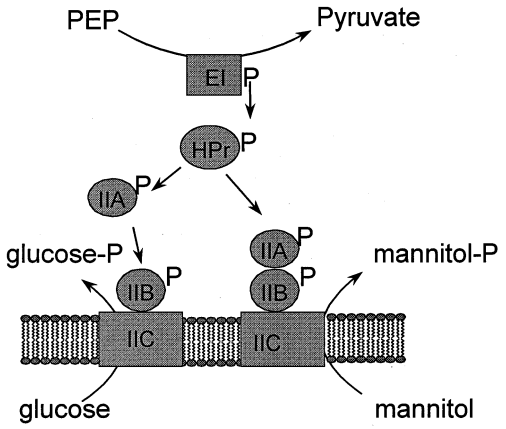

Fig. 1. Schematic representation of the mannitol-specific and the glucose-specific phosphoenolpyruvate-dependent phosphotransferase systems as found in *E. coli*.

The degree of attention paid to each activity depends on the EII investigated.

2. General organization and disposition in the membrane

All EIIs are organized into protein units or domains. The units responsible for transport (the C domain and, in some cases, a D domain) are situated in the cytoplasmic membrane, while those responsible for transferring the phosphoryl group to the incoming carbohydrate (the A and B domains) are situated in the cytoplasm and may or may not be linked to the membrane-bound domains or to each other.

2.1. EII^{glc}

EII^{glc} in *Escherichia coli* consists of two proteins IIA^{glc} and $IICB^{glc}$. The phosphorylation sites are H90 and C421 in the A and B domain, respectively [5]. $IICB^{glc}$ is functional as a dimer and is specific for glucose and methyl-α-D-glucopyranoside (α-MG). The K_d of glucose is 1.5 μM [6]. Although the B domain is able to carry out phosphoryl transfer from C421 to glucose, the process is stimulated by the presence of IIA^{glc} suggesting that a IIA^{glc}:$IICB^{glc}$ complex occurs; this has been verified by immunoprecipitation [7]. A proposal for the organization of the peptide chain in the membrane, based on hydropathy analysis plus PhoA and LacZ protein fusions suggests the occurrence of eight *trans*-membrane helices (TMHs) and a large hydrophilic loop of 70 amino acids between TMH VI and VII at the cytoplasmic side of the membrane (Fig. 2A) [8]. A highly conserved GIXE sequence, which might be involved in substrate binding [9], is located in TMH VII at the periplasmic side.

2.2. EII^{mtl}

EII^{mtl} in *E. coli* consists of one protein in which the two cytoplasmic domains, A and B, and the membrane-embedded C domain are linked together giving $IICBA^{mtl}$. It is only functional as a dimer and has, per dimer, one high- and one low-affinity binding site for mannitol in the nanomolar and micromolar concentration ranges [2]. The crucial contacts between the subunits are between the C domains [10,11]. Stable heterodimers can be formed, both in vivo, by co-expressing two mutant forms of the protein and in vitro, by mixing mutant forms of the protein, solubilized by a PEG-based detergent (see Section 5). Although the hydropathy plot of IIC^{mtl} is similar to that for IIC^{glc}, protein fusion experiments suggest the occurrence of only six TMH (see Fig. 2B) [12]. One indication that one of these schemes may have to be corrected is that the highly conserved GIXE sequence is situated, in the proposed II^{glc} structure, in TMH VII near the periplasmic side of the membrane while, in the proposed II^{mtl} structure, it is located in a large cytoplasmic loop between TMH IV and V.

2.3. EII^{man}

The *E. coli* PTS mannose transporter consists of $IIBA^{man}$ and the two membrane-bound subunits IIC^{man} and IID^{man}. $IIBA^{man}$ forms homodimers with phosphorylation sites at H10 and H175 on the B and A domains, respectively [13]. It is water-soluble but associates reversibly with the membrane-bound part with a K_d of 5–10 nM [14]. IIC^{man} and IID^{man} are tightly associated and cannot be expressed separately in a functional form [15]. The substrate binding site is situated in the C domain [14]. Besides functioning as transporters for mannose, glucose and related hexoses, the membrane-bound C and D domains also play a role in the transfer mech-

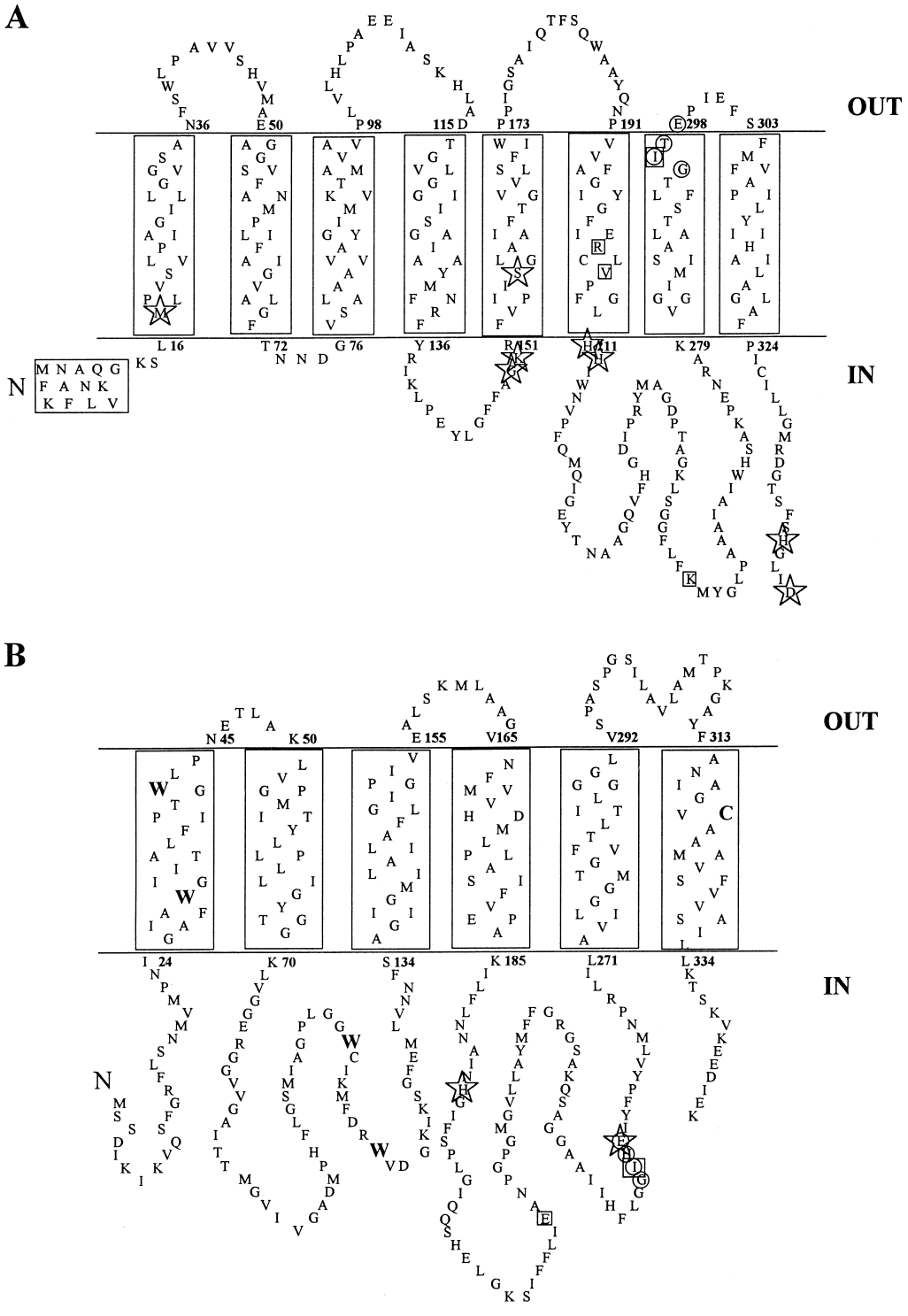

anism for the infection of *E. coli* by phage λ DNA [16]. The topologies of IIC^{man} and IID^{man} have been determined by protein fusion [17]. Six TMH were predicted for the 27 kDa C domain with both the C- and N- termini located on the cytoplasmic side. The 31 kDa D domain is anchored in the membrane at its C terminus by only one TMH with the remaining 260 residues situated in the cytoplasm. A subunit

Fig. 2. Transmembrane distribution of residues in the membrane-bound domain of: (A) *E. coli* EII^{glc} [8]. The residues participating in the highly conserved GIXE sequence are encircled. Residues in EII^{glc} which, when mutated, result in substantially lower transport activity and somewhat reduced in vitro phosphorylation activities are marked with a star. Residues in EII^{glc} which, when mutated lead to transport even in the absence of phosphorylation (facilitated diffusion), are marked with a square. Note that one of these residues is the encircled I296, part of the GIXE motif. When the same mutation was made in EII^{mtl} facilitated diffusion was also observed [27]. (B) *E. coli* EII^{mtl} [12]. The residues participating in the conserved GIXE sequence are encircled. Residues in EII^{mtl} which, when mutated, result in transport without phosphorylation are enclosed in boxes. Those which demonstrate second site suppression are marked with stars. The tryptophans and C320 subjected to fluorescence spectroscopy are enlarged and highlighted in bold type.
←

stoichiometry of $IIBA_2^{man}$ IIC_1^{man} IID_2^{man} was determined for this complex [15]. Freeze fracture electron microscopy of the IIC/IID complex reconstituted in proteoliposomes gave a molecular mass of 100 ± 20 kDa, in good agreement with the proposed subunit stoichiometry of IIC_1^{man} IID_2^{man} (90 kDa).

3. The kinetic and mechanistic aspects of domain interactions in phosphoryl group transfer and transport

3.1. Artificial domain fusion

In order to obtain deeper insight into the kinetic effects of covalent coupling between domains, Mao et al. fused all four proteins participating in the phosphoryl transfer from PEP to glucose to produce a 150 kDa complex linked in the order H_2N–$IIBC^{glc}$–IIA^{glc}-HPr-EI [18]. An Ala–Pro-rich 20 amino acid linker was employed similar to that found in the *E. coli* $IIBA^{man}$ and in the multi-phosphoryl transfer protein of the *Rhodobacter capsulatus* fructose PTS comprising HPr, EI and IIA. The fused protein showed transport activity in vivo but the purified protein was only 3–4 times more active in glucose phosphorylation than a mixture of the separate proteins at the same concentration. Based on the much higher local concentration of active sites, one would have expected a much higher specific activity for the fused protein compared to the mixture of separate domains. Steric effects caused by the introduction of the linkers could be responsible for the modest increase in specific activity. Such a possibility recently gained credence when Lanz and Erni substituted α-helix-favoring alanine residues for the original β-sheet-favoring Thr and Gly residues in a conserved portion of the linker between the B and C domain of *E. coli* II^{glc}. The substitutions reduced the rate of in vitro α-MG phosphorylation to between 1 and 10% that of the wild-type protein [19]. The pathway of phosphoryl transfer from HPr to IIA^{glc} in the fused H_2N–$IICB^{glc}$–IIA^{glc}–HPr–EI complex appears to be restricted to the fused components since introduction of free $IIBA^{man}$, IIC^{man}, IID^{man} and the substrate deoxyglucose did not result in phosphorylation of this carbohydrate, as it should have if the covalently-linked HPr were able to donate its phosphoryl group to proteins outside the covalent complex. Similarly, the addition of EI, HPr, or IIA^{glc} did not result in a higher α-MG phosphorylation activity, showing that the phosphoryl group can also not be funneled into the fused protein from phosphoryl donors free in solution. Both results are surprising in light of observations with different EIIs that domain complementation between naturally fused proteins and extraneous domains readily occurs both in vivo and in vitro.

3.2. A/B domain complementation

Domain complementation was first offered as an explanation for the observation that α-MG phosphorylation activity was observed with $IICB^{glc}$ even in the absence of IIA^{glc}, if *E. coli* $IICBA^{nag}$, $IICBA^{bgl}$ or *Klebsiella pneumoniae* $IICBA^{nag}$ were present [20]. Similarly, truncated $IICB^{nag}$ from *K. pneumoniae* could be complemented by IIA^{glc} [21]. The A domains of all three proteins are highly homologous to *E. coli* IIA^{glc} and, even when covalently attached to their natural B domain phosphoryl group acceptors, are still able to phosphorylate an extraneous B domain or CB complex. In the case of the mannose PTS, mixing H10Q–$IIBA^{man}$ and H175Q–$IIBA^{man}$, each inactive by virtue of a mutation in the B and A domain phosphorylation site, respectively, resulted in an active system [4]. The mannitol PTS also shows complementation; a truncated EII^{mtl} lacking the en-

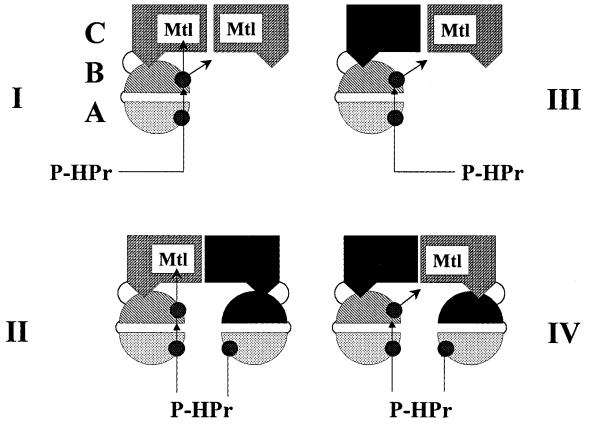

Fig. 3. Possible routes of phosphoryl transfer in heterodimers of EII^{mtl}. A blackened domain indicates that it is inactive by virtue of a mutation. (I) A wild-type subunit combined with IIC^{mtl}. Phosphoryl transfer can proceed along one subunit or across the domain interface from the B domain of one subunit to the C domain of the adjacent subunit. (II) A wild-type subunit combined with a mutant protein which is incapable of being phosphorylated on the B domain or binding mannitol to the C domain. (III) C domain mutant protein which is inactive in binding mannitol combined with IIC^{mtl}. Phosphoryl group transfer can only occur across the subunit interface. (IV) C domain mutant protein combined with a B domain mutant protein.

tire A domain and thus its H554A phosphorylation site, could be complemented by a $IICBA^{mtl}$ whose B domain phosphorylation site, C384, had been inactivated by NEM alkylation [22]. Related to this, mixing the C384S and H554A mutants, restored the PEP-dependent mannitol phosphorylation activity up to 55% of the wild-type activity [23]. The above experiments pertain only to in vitro phosphorylation activity. Weng et al. demonstrated that domain complementation also occurs in vivo and is able to restore phosphorylation-coupled transport activity as well. Heterodimers formed by the in vivo coexpression of inactive C384H-EII^{mtl} with H554A-EII^{mtl} or C384H-EII^{mtl} with H554D-EII^{mtl} mutants yielded cells able to grow on and ferment mannitol [24].

3.3. B/C domain complementation

Complementation of various inactive mutants of EII has been investigated to address mechanistic and kinetic aspects of subunit interactions in phosphoryl group transfer and carbohydrate transport. Boer et al. performed in vitro complementation experiments using purified wild-type EII^{mtl}, IIC^{mtl}, C384S, G196D and the double mutant C384S:G196D [25]. If the phosphoryl group had to proceed from the B domain of one subunit to mannitol bound at the C domain of another subunit, as in scheme III and IV of Fig. 3, approximately 10-fold lower mannitol phosphorylation activity was observed [24,26,27]. On the other hand, activities comparable to that of the wild-type homodimer were observed if active wild-type EII^{mtl} was mixed with an excess of one of the inactive mutants or IIC^{mtl} (scheme I and II in Fig. 3). In these heterodimers, the phosphoryl group can transfer within one wild-type subunit; it does not have to cross the subunit interface to bypass a mutation in one of the domains. We conclude, therefore, that the capacity of one wild-type subunit in an EII^{mtl} heterodimer is sufficient for efficient phosphoryl transfer from P-HPr to mannitol. Uptake experiments confirmed this view since coexpression of wild-type EII^{mtl} with overproduced levels of G196D or the G196D:C384S double mutant resulted in comparable uptake activities as found with vesicles containing only wild-type EII^{mtl} [25].

Jacobson and colleagues reported that the C domain EII^{mtl} mutations, H195R, H195A and H195N

Table 1
Comparison of transport phenotypes and phosphorylation rates for EII^{mtl} mutants[a]

	K_d (μM)	PEP-dependent phosphorylation rate (nmol mtl-1-P/min/mg membrane protein)
Wild-type	0.042	50
H195N	2.7	25
H195A	3.4	<3
H195R	3.0	<3
	Phenotype[c]	
Wild type	Red	26
H195A/H554A	Red	3
H195A/H554D	Red	2.5
H195R/C348H	White	<0.2
H195A/C384H	White	n.d.[b]

[a]Data taken from [26].
[b]n.d., not determined.
[c]A red phenotype indicates transport and fermentation of mannitol; a white phenotype indicates lack of fermentation and usually lack of transport.

all resulted in a 65–80-fold higher K_d for mannitol compared to the wild-type enzyme (Table 1) [24,26]. H195R and H195A were inactive in phosphorylation of mannitol while H195N had a V_{max} value of 50% compared to wild-type activity. Coexpression yielding H195A/H554A or H195A/H554D heterodimers resulted in a PEP-dependent phosphorylation activity in permeabilized cells which was 10% of that found in cells expressing wild-type enzyme, but no activity was observed for H195A/C384H or H195R/C384H heterodimers under these conditions [26]. Since they found high phosphorylation activity with the E257A/C384H heterodimer, they concluded that different subunits in the heterodimer could contribute E257 and C384 and still complement but that H195 and C384 must be situated on the same subunit and interact with each other during the catalytic cycle [27]. Boer et al. reached the opposite conclusion with an in vitro study on a comparable mutant combination, G196D/C384S instead of H195R/C384H. They reported a phosphorylation activity roughly 10% that of wild-type enzyme, suggesting that C384 and G196 could be contributed by different subunits in the heterodimer [25]. The discrepancy between these two studies could arise from the differences in the specific amino acid replacements or from the procedure used to measure phosphorylation activity. In the latter case, activity was measured in vitro, with a large excess of one of the mutant proteins over the other in order to obtain the maximum amount of heterodimer; this would facilitate measuring a low specific activity, if present, in the heterodimer. In the former case, activities were measured in permeabilized cells with no attempt to alter the relative populations of the mutant proteins.

Lanz and Erni have examined B/C domain complementation in *E. coli* EII^{glc} while focusing on residues that are conserved in the B and C domain of the glucose EII family [19]. These include R424 and R426 in the phosphorylation site loop of the B domain and H211 and H212 in the large cytoplasmic loop of the C domain. R→K mutations in these B domain residues inactivated both in vivo transport of α-MG and in vitro phosphorylation of glucose because the mutant proteins, although they could be phosphorylated on C421, were unable to pass the phosphoryl group to the carbohydrate bound to the C domain. H212Q-EII^{glc} was inactive in glucose transport and fermentation in intact cells, whereas the H211Q mutant protein retained enough activity to support measurable growth and fermentation on glucose; it also retained 10% of the wild-type α-MG transport activity. Both mutants could still bind and phosphorylate glucose in in vitro phosphorylation assays but with different reduced activities. Complementation of glucose in vitro phosphorylation activity was demonstrated with the H212Q/R424K, H212Q/R426K, H211Q/R426 and H211Q/C421S purified protein pairs.

B/C domain complementation seems to be firmly established but what physical picture we should associate with such a process is still uncertain. Since both $IICB^{glc}$ and $IICBA^{mtl}$ function as dimers, the simplest picture would be one where each monomer retains its internal architecture and the phosphoryl transfer from the B domain of one mutant to the C domain of the other entails crossing the subunit interface, at least in these complementing mutant proteins. The other possibility is that domains from the separate monomers interchange so that one complete active unit is formed. It is even possible that this is the normal architecture for EII dimers, i.e., that they are constructed by the intertwining of the monomer domains. The X-ray crystal structure of *E. coli* $IIBA^{man}$ dimer shows such an arrangement (see section 8.2)

3.4. C/C domain complementation

Glutamate 257 in the GIXE sequence has been replaced in EII^{mtl} with an alanine, glutamine or aspartic acid [26,27]. The E257A and E257Q mutants showed no affinity for mannitol while the E257D bound mannitol with only low affinity ($K_d = 11$ μM). The latter mutant also possessed PEP-dependent phosphorylation activity with a V_{max} value which was 70% of the wild-type activity but mannitol uptake activity which was only 3% that of wild-type enzyme. Clearly, mannitol phosphorylation and translocation occur at different rates with this mutant. The most intriguing result to date with C domain mutants is that, while E257A-EII^{mtl} and H195A-EII^{mtl} are both inactive in transport and in vitro phosphorylation, a heterodimer composed of two the mutants is active. Coexpression of the two proteins yielded a heterodimer with a reduced but

measurable in vivo mannitol transport, a K_m for in vitro mannitol phosphorylation comparable to the wild-type protein and an in vitro phosphorylation activity which was 20% that of the wild-type enzyme (Table 2). This is the first reported case of second-site suppression involving mutations in the two C domains of the EII^{mtl} dimer, suggesting that these regions may be involved in forming a common mannitol binding site and/or translocation pathway.

The complementation studies with EII^{mtl} lead to the following conclusions.

- EII^{mtl} can form stable heterodimers both in vivo and, when the enzymes are solubilized in a PEG-based detergent, in vitro.
- The preferential route of phosphoryl group transfer from HPr to mannitol is along a single subunit in the dimer. Furthermore, only one subunit is used per dimer to phosphorylate mannitol. This might be directly related to the observation that only one high affinity mannitol binding site is present per dimer.
- The PEP-dependent EII^{mtl} activity is hardly affected if the phosphoryl group is forced to cross the A/B domain interface in the heterodimer; however, phosphoryl transfer across the B/C heterodimer interface significantly affects the enzyme activity and is strongly dependent on the point mutation inactivating the C domain. Whether this is also true for point mutations inactivating the B domain has not yet been investigated.
- Second site suppression has been demonstrated by combining proteins inactive due to mutations at positions in the large cytoplasmic loop. Consequently, residues in this region may form the dimer interface and a common mannitol binding and translocation site.

4. The mechanism of coupling phosphorylation and transport

Phosphorylation plays two roles in EII function: (i) movement of the carbohydrate from the periplasmic to the cytoplasmic binding site on EII, and (ii) release of the carbohydrate as carbohydrate-phosphate from the cytoplasmic binding site. The occurrence of mutant EIIs which carry out only one or the other process confirms that the two activities are dis-

Table 2
Comparison of EII^{mtl} C domain mutant kinetic characteristics[a]

	Mannitol binding[b]		PEP-dependent mannitol phosphorylation[b]		Mannitol uptake[c]	
	K_d (μM)	K_d (nM)	K_m (μM)	V_{max}	K_m (μM)	V_{max}
Wild-type	5.2	60	17	44	33	550
E257A	ND[e]	ND	ND	ND	ND	ND
E257Q	ND	ND	ND	ND	ND	ND
E257D	11	ND	25	30	100	15
H195N	2.7	ND	31	25	56	67

	PEP-dependent mannitol phosphorylation[d]		Phenotype[f]
	K_m (μM)	V_{max}	
Wild-type	25	225	Red
E257A/H195A	35	50	Pink

[a]Data taken from [27].
[b]Measurements done on membrane vesicles.
[c]Measurements done on whole cells.
[d]Measurements done in permeabilized cells. The V_{max} and K_m values for vesicle preparations and permeabilized cells differ.
[e]ND, not detectable.
[f]A red phenotype indicates transport and fermentation of mannitol; a pink phenotype indicates low levels of transport and/or fermentation.

tinguishable. These mutant proteins have been dubbed 'uncoupled' EIIs because there is no longer a mechanistic link between the two processes.

4.1. Coupling at the level of substrate phosphorylation

EII catalyzes the conversion of the carbohydrate substrate to carbohydrate-P once the substrate has reached the cytoplasmic binding site either by transport from the periplasmic site or by binding to the cytoplasmic site directly from the cytoplasm. Since the affinity of the phosphorylated product is four to six orders of magnitude weaker than the non-phosphorylated substrate, a minimal mechanism of coupling of phosphorylation and transport could be simply the chemical conversion of a high affinity substrate into a low affinity product resulting in the release of the transported substrate from the cytoplasmic binding site. At this level, one might expect to find uncoupled EIIs which release their substrate from the cytoplasmic binding site before they become phosphorylated. In general, these would be mutant EIIs whose cytoplasmic binding sites had significantly lower affinities for the non-phosphorylated carbohydrate. Since they were uncoupled, the rates of transport could be different from the rates of phosphorylation.

Buhr et al. reported a series of transport-deficient $IICB^{glc}$ mutants with expression levels comparable to wild-type enzyme [28]. The mutations, M17T, M17I, G149S, K150E, S157F, H339Y and D343G were located in three protein segments in the C domain (see the residues marked by stars in Fig. 2A). M17 is predicted at the cytoplasmic side of TMH I, the most conserved helix in the EII family [3]. The residues around position 150 are located at the beginning of TMH V while position 339 and 343 are situated on the C-terminal side of TMH VIII. The mutant proteins retain less than 5% of the wild-type α-MG transport activity and 20–40% of the glucose transport activity. The residual phosphorylation activity, on the other hand, varied between 20–70% for α-MG and 40–100% for glucose. The H211Q mutant of Lanz and Erni also falls into this category [19]. The H212Q mutant is a more extreme case in that the transport activity is so low that it cannot be measured and the phosphorylation activity is much more impaired than in H211Q, but still measurable. Apparently, these mutant proteins are impaired in their transport function more than in their phosphorylation function. Ruijter et al. isolated four *E. coli* $IICB^{glc}$ mutants capable of transporting in the absence of phosphorylation. To do this, they introduced a plasmid encoding *E. coli* $IICB^{glc}$ into a *Salmonella typhimurium* strain lacking EI and HPr and $IICB^{glc}$ [6]. The mutations R203S, V206A, I296N and K257N resulted in proteins which allowed wild-type growth on glucose, thus transport, even though phosphorylation by the PTS was impossible. These positions are located in TMH VI and VII and the cytoplasmic loop between them. I296 is part of the conserved GIXE sequence. With the exception of the K257N mutant, these enzymes were also able to phosphorylate glucose and α-MG. Although the extent of coupling between the phosphorylation and transport activity has not been determined in detail, these two studies clearly show that the coupling can be relaxed significantly by single mutations.

EII^{man} has been reconstituted in proteoliposomes in order to study the coupling between the transport and phosphorylation [14]. No facilitated diffusion of glucose could be detected suggesting that, in this system, with this carbohydrate, the coupling between transport and phosphorylation of the carbohydrate was absolute. The turnover rate for the vectorial phosphorylation activity was 72 min^{-1} while that for the non-vectorial activity was 2–3-fold higher. Since the non-vectorial phosphorylation activity did not cross-inhibit the vectorial phosphorylation activity, one must conclude that either the two processes are mechanistically separate, or that the return of the empty carbohydrate binding site to the periplasmic side is much faster that the binding of carbohydrate from the cytoplasmic space.

4.2. Coupling at the level of transport

In addition to coupling phosphorylation to transport by driving the release of substrate once it reached the cytoplasmic binding site, phosphorylation could also be coupled to transport by driving the movement of the substrate from the periplasmic to the cytoplasmic binding site. Events related to the movement of mannitol between these two sites have been investigated in detail by both steady-state and pre-steady-state kinetics using purified protein recon-

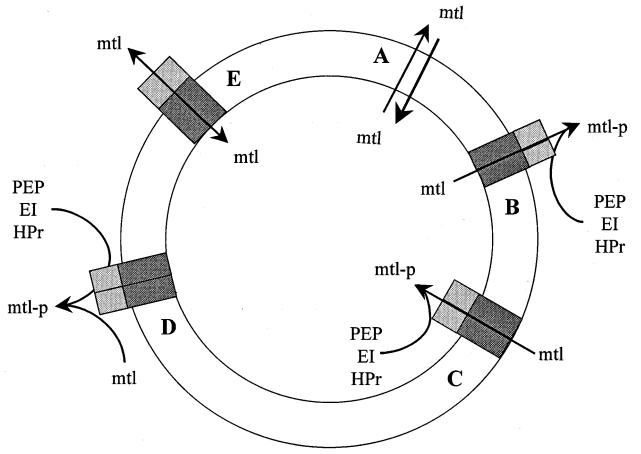

Fig. 4. A schematic representation of the reactions observed to occur in proteoliposomes containing randomly oriented EII^{mtl} [29]. (A) Passive diffusion; (B) vectorial efflux; (C) vectorial accumulation; (D) non-vectorial phosphorylation; (E) facilitated diffusion.

stituted in proteoliposomes or using right-side-out (RSO) and inside-out (ISO) vesicles as the source of EII^{mtl}.

EII^{mtl} reconstituted into proteoliposomes orients with the cytoplasmic domains facing inward as well as outward. EII^{mtl}-catalyzed facilitated diffusion of mannitol over the membrane was slow but measurable using a mannitol concentration gradient of 10. Active transport could easily be studied either by making use of the properly oriented EII population and measuring the rate of mannitol uptake in proteoliposomes pre-loaded with PEP, HPr and EI or by making use of the inverted population of carriers, trapping [^{3}H]-mannitol on the inside, adding PEP, HPr and EI to the outside and monitoring the PEP-dependent efflux rate (see Fig. 4) [29]. The mannitol transport rate was measured to be 243 min^{-1}, two orders of magnitude higher that found for the unphosphorylated enzyme (facilitated diffusion), demonstrating a mechanistic coupling between the phosphorylation and transport activity. Experimental difficulties prevented an accurate measurement of the K_m for mannitol in the transport process but it was at least lower than 10 μM. When non-vectorial phosphorylation was measured by adding all components, PEP, EI, HPr and mannitol to the outside of the proteoliposomes and monitoring the mannitol-P formed, also at the outside, the rate of phosphorylation was found to be at least a factor of 10 higher than the rate of transport. The affinity for mannitol, however, was much lower. Fig. 4 summarizes the processes which are catalyzed by EII^{mtl} reconstituted in proteoliposomes. Vectorial transport (Fig. 4B,C) occurs with a relatively low rate while non-vectorial phosphorylation (Fig. 4D) is characterized by a 10-fold higher rate. The periplasmic-facing binding site is high affinity while the cytoplasmic-facing binding site is characterized by a 10-fold lower affinity.

The extent of coupling (the number of mannitol transport events per mannitol phosphorylation events) was determined by mannitol-1-phosphate burst experiments, using ISO vesicles equilibrated with [^{3}H]mannitol which were mixed with P-HPr [30]. After transport from the periplasmic side to the cytoplasmic side, 45% of the bound [^{3}H]mannitol can be trapped as [^{3}H]mannitol-1-phosphate. The other part is released in the cytoplasmic space where it can be rebound and phosphorylated in another round. Apparently, the release of mannitol from E_{cyt} occurs at a rate comparable to the phosphoryl transfer rate so that the transport and subsequent phosphorylation of mannitol can be viewed as consecutive and independent reactions [3,31]. This being the case, one should be able to find mutants in which one of the reactions is impaired. The G254E mutant shows phosphorylation but no transport activity. The E218A and E218V mutants allow facilitated transport of mannitol while the phosphorylation activity is drastically reduced [3]. All these mutations are located in the large cytoplasmic loop between TMH IV and V.

Flow dialysis was used to investigate the individual steps in the mannitol binding process with both ISO and RSO vesicles. Mannitol binds with a high affinity K_d of 40 nM to both preparations. At room temperature, binding is complete within the dead-time (6 s) of the flow dialysis apparatus. The exchange of [^{3}H]mannitol bound to RSO vesicles for free [^{1}H]mannitol is also complete in the dead-time but, in the case of ISO vesicles, exchange is complete only after 6 min. This slow exchange rate can be attributed to an additional step, besides binding, involved in the exchange process. It becomes visible at 4°C, even in the binding process, as two-phase binding kinetics, a relatively fast mannitol concentration-dependent binding step and a slower mannitol concentration-independent binding step [32]. The latter

process with a rate constant of 0.14 min^{-1} has been attributed to the recruitment of binding sites to the cytoplasmic side (E_{cyt}) from an occluded state which appears to be the equilibrium state (E_{equi}). The equilibrium constant $K = E_{equi}/E_{cyt}$ is 2.1 ± 0.5 min^{-1}. If state E_{equi} was also in equilibrium with the binding site at the periplasmic side (E_{per}), one would expect an equal concentrations of bound mannitol after equilibration with EII^{mtl} either in ISO or RSO vesicles. However, significantly more mannitol was bound by ISO than by RSO vesicles proving that E_{equi} cannot be reached from the periplasmic side at 4°C. Lowering the temperature appears to dramatically decrease the isomerization rate between the different enzyme states and thus the mannitol dissociation rate constant. This can explain the strong dependence of the K_d value on temperature [33]. Data collected so far are in agreement with a model in which the high affinity binding site isomerizes between E_{per} and E_{cyt} via an occluded state, E_{equi}. Additional experiments are needed to determine whether this is also the case for the low-affinity binding site and whether there is a cooperative interaction between these sites. While isomerization between E_{cyt} and E_{equi} occurs at a measurable rate even in the absence of phosphorylation of the B domain at C384, this is not the case of the isomerization between E_{per} and $E_{equi.}$ Consequently, the energy coupling step in the actual transport process is the phosphorylation-driven lowering of the activation energy for the conversion of the E_{per}:mannitol complex to the E_{equi}:mannitol complex. Since the phosphorylation event itself occurs on the B domain which can be physically separated for the C domain, the energy coupling process is one of conformational coupling.

5. Changes in the oligomeric state of EII^{mtl} induced by detergents

Unraveling details of the A/B and B/C domain interactions have, in part, relied on experiments involving the formation of heterodimers from purified enzyme. In the case of EII^{mtl}, the nature of the detergent plays a decisive role in this process. EII^{mtl} is present as a dimer in *E. coli* vesicles and when solubilized in a number of detergents including decyl-PEG [10,34]. In this detergent, EII^{mtl} shows a mannitol phosphorylation activity comparable with that in *E. coli* vesicles [35], implying that decyl-PEG is an excellent detergent for the study of EII^{mtl}. We recently discovered, however, that reversible inactivation can take place in PEG-based detergents. Experiments designed to study this effect have led to a new level of understanding and control of the association characteristics of EII^{mtl} [36]. Upon heating PEG-based detergent solutions, the PEG chains become partly dehydrated, resulting in stronger van der Waals interactions between micelles which induce micelle cluster formation. The cluster size increases as a function of temperature until, at a certain temperature, the cloud-point or demixing temperature (T_d), the clusters become large enough to cause significant light scattering and the solution becomes turbid [37]. The micellar cluster size increases asymptotically and follows a power-law given by $(T_d - T)/T_d$ [38]. Thus, at a temperature just below T_d, large clusters are present in a homogeneous solution. Variation of the cluster size at a fixed temperature can be generated by the introduction of dehydrating agents like Na_3PO_4 or NaF [37]. Increasing the concentration of these salts results in a linear decrease of T_d and an increase in cluster size since $(T_d - T)/T_d$ is increased. The increase in hydrodynamic radii (R_h) of the micelle clusters can be visualized by dynamic light scattering. In the case of EII^{mtl}, the following observations have been made. The T_d of pure decyl-PEG in assay buffer is 58°C. Adding up to 250 mM Na_3PO_4 decreased the T_d to 33°C. and resulted in a 85% lower enzyme activity [36]. The enzyme inactivation could be completely reversed if the enzyme was diluted again in a buffer with a high T_d. One explanation for the reversible inactivation could be a change in EII^{mtl} oligomeric state from active dimers to inactive monomers [39]. If this were the case, lower T_d and higher enzyme concentrations would be expected to produce a larger fraction of dimers due to mass action. This has been confirmed experimentally suggesting indeed that micelle clustering induces monomerization of the enzyme. The rate of formation of active heterodimers upon mixing two inactive enzymes, IIC^{mtl} and G196D-EII^{mtl}, was also affected by the micelle cluster size. The rate was much faster at lower T_d or increased micelle cluster size suggesting that the dissociation of homodimers is the rate-determining step in the formation of heterodimers.

Similar results were obtained if the enzymes were incubated with mannitol, a compound known to monomerize EII^{mtl} [40].

The monomerization of EII^{mtl} upon clustering of micelles can be rationalized as follows. The microenvironment of PEG-based detergent micelles becomes less polar with increasing dehydration and increasing micelle cluster size [37,41,42]. Since hydrophobic bonding is known to be involved in the dimerization of EII^{mtl}, a less polar environment, like large micelle clusters, will reduce the driving force for hydrophobic bonding, resulting in monomerization of EII^{mtl} [43,44]. No heterodimer formation between IIC^{mtl} and G196D-EII^{mtl} could be induced in buffers containing decylmaltoside, a detergent in which micelle clustering does not occur. A PEG-based detergent and micelle clustering appears to be necessary for efficient EII^{mtl} heterodimer formation. Whether this is also true for other membrane proteins including other EIIs has yet to be determined.

6. The thermodynamics of domain interactions

Although the mechanistic relevance of A/B domain interactions is not yet clear, B/C or B/CD domain interactions play a pivotal role in the mechanism of carbohydrate translocation by the membrane-bound domain, as has been demonstrated for EII^{mtl}, EII^{glc} and EII^{man} [14,28–30]. Experiments with separately expressed and purified IIB^{glc} and IIC^{glc} revealed that P–IIB^{glc} itself was not able to bind and phosphorylate α-MG. The phosphoryl transfer from IIA^{glc} was faster to IIB^{glc} than to $IICB^{glc}$, while the dephosphorylation half-life at 21°C of P–IIB^{glc} was 40 h versus 9 h for P–$IICB^{glc}$ [43]. This result clearly shows that the C domain influences the microenvironment of Cys421 at the B domain. The interaction, however, must be a loose one since IIB^{glc} can transfer its phosphoryl group to glucose bound by C412S $IICB^{glc}$. The specific activity of IIC^{glc} in the presence of a 100-fold excess IIB^{glc} was 50 times lower than for $IICB^{glc}$. A comparable relative activity was reported when the activity of the three separate domains of $IICBA^{mtl}$ was compared with the wild-type enzyme [44]. In both enzymes, the B and C domains exhibit a low affinity for each other.

6.1. Differential scanning calorimetry

Calorimetric techniques have been applied to provide a complete thermodynamic description of the domain interactions, ΔH, ΔS, ΔG and the effect of domain phosphorylation and substrate binding on these parameters [33,45,46]. For this purpose, measurements were made on the individual EII^{mtl} domains as well as pairwise combinations, all of which were fully active in vivo and in vitro. The unfolding of IIA^{mtl}, IIB^{mtl}, IIC^{mtl}, $IIBA^{mtl}$ and $IICB^{mtl}$ was investigated with differential scanning calorimetry (DSC) [46]. This technique registers the heat associated with protein unfolding as a function of temperature and yields the midpoint temperature of the unfolding transition, T_m, and the enthalpy of unfolding, ΔH. Using the individual domains as reference states, differences in T_m or ΔH measured for the domain combinations can be related to interactions occurring at the domain interface or changes in the individual domains as a result of these interactions. The most straightforward studies done on EII pertain to the soluble A and B domains. The ΔH and T_m of the B domain unfolding decreased both in $IIBA^{mtl}$ [33] and $IIBA^{man}$ [47] relative to that in the absence of the partner A domain. This could indicate that the presence of the A domain destabilizes rather than stabilizes the B domain. A more likely explanation is that changes in ΔH are compensated by changes in ΔS, enthalpy–entropy compensation, due to solvent rearrangement resulting from the domain interactions, such that the change in ΔG is favorable. Irrespective of the directions of the changes in ΔH, the absolute value of the ΔH for IIB^{mtl} as well as for the B domain in the $IIBA^{mtl}$ protein, are the lowest found in the literature for a protein of this size. This issue resurfaces again in our consideration of C/B domain interactions.

The effect of phosphorylation on A and B domain stability and A/B domain interaction could not be monitored by DSC since EI used to phosphorylate the A domain inactivates upon heating during the DSC measurement. Instead, guanidine hydrochloride (GuHCl) was used as the denaturant and the unfolding was monitored by changes in CD at 222 nm. Phosphorylation destabilized the IIA^{mtl} and the A domain in $IIBA^{mtl}$ to approximately the same extent but had no effect on the IIB^{mtl} or the B domain in

$IIBA^{mtl}$. Since, in the doubly phosphorylated form, P_2–$IIBA^{mtl}$, the midpoints of unfolding for the P-A and P-B domains were almost identical, no information could be extracted about the free energy of unfolding, associated with A/B domain interactions. Given that the A domain phosphorylation site is situated in a hollow on the surface of the protein surrounded by hydrophobic side chains (see Section 8.3) while the B domain phosphorylation site is more exposed on the surface of the protein, the destabilizing effects of phosphorylating the A domain may be due to alteration of the hydration in the active site by introduction of the charged phosphoryl group. In conclusion, the $IIBA^{mtl}$ and $IIBA^{man}$ studies demonstrate that A/B domain interactions are present, both in the non-phosphorylated and phosphorylated protein; however, in both systems these interactions must be evaluated in a larger context since both proteins are either covalently attached to, or strongly bound to, their membrane-bound partners.

C/B domain interactions were studied with EII^{mtl} reconstituted in dimyristoyl phosphatidylcholine (DMPC). Since the presence of protein disturbs the lipid order, it lowers the T_m of the lipid phase transition. From this data, it could be calculated that approximately 40 lipid molecules are associated with a IIC^{mtl} monomer [46]. A comparable value has been found in case of bacteriorhodopsin, a protein with a membrane domain similar in size to IIC^{mtl} [48]. The thermal unfolding of reconstituted EII^{mtl} in DMPC vesicles was studied in the presence of 100 μM mannitol. Two transitions were observed with peaks around 62°C and 82°C. Only the low-temperature transition was observed for $IIBA^{mtl}$ while the unfolding of IIC^{mtl} gave a single transition at 76°C. Deconvolution of the low-temperature transition resulted in two overlapping transitions from the A and B domains. The presence of mannitol had no effect on the unfolding of the A and B domains but it strongly influenced the unfolding of the C domain. The T_m and ΔH of the C-domain transition in $IICBA^{mtl}$ were substantially lower in the absence versus the presence of mannitol. Unfolding of a duplicate sample after trypsin treatment showed that removal of the B domain resulted in an even lower ΔH of unfolding of the C domain. Apparently, part of the B domain is still able to stabilize the C domain even after passing the 59°C T_m of its own unfolding transition. In the presence of mannitol, the T_m of the C domain in $IICBA^{mtl}$ increases by 5°C and ΔH increases by 100 kJ/mol while these values increase only 3°C and 20 kJ/mol, respectively, after trypsin digestion. Thus, the presence of mannitol strengthens the stabilizing effect of the B domain on the C domain, even at temperatures where the B domain is unfolded and the C domain starts to unfold.

6.2. Isothermal titration calorimetry

The thermodynamic parameters associated with mannitol/EII^{mtl} interactions were derived from isothermal titration calorimetry (ITC) data [33]. These experiments were performed with *E. coli* ISO vesicles overexpressing EII^{mtl}. The change in heat, ΔH^o_{obs}, upon titration of substrate to a vesicle suspension yields the stoichiometry of binding and the dissociation constant, K_d, and, therefore, ΔG^o_{obs}. The dependence of ΔH^o_{obs} on the temperature yields ΔCp^o_{obs}, a measure for the changes in hydration energy of amino acid side chains during the binding event [49]. The titration curves could be properly fit by a one-set-of-sites model giving 0.67 sites per monomer with a K_d of 115 nM, values in agreement with flow dialysis data. By performing the experiments at four different temperatures between 10°C and 25°C, a ΔCp^o_{obs} of -4.0 ± 0.3 kJ K^{-1} mol^{-1} was found. The ΔCp^o_{obs} is large compared with ΔCp^o_{obs} values for other enzyme/substrate interactions e.g., serine with the serine receptor of bacterial chemotaxis [50] or binding of glucose to yeast hexokinase (ΔCp^o_{obs} are -0.7 and -0.2 kJ K^{-1} mol^{-1}, respectively) [51]. A similar ΔCp^o_{obs} was found for perseitol, a mannitol analogue which cannot be translocated or phosphorylated [52]. Spolar and Record correlated the ΔCp^o_{obs} values for a variety of systems of known 3D structure, with the changes in these structures upon binding ligands or altering association states [49]. Their analysis resulted in an average value for ΔCp^o_{obs} upon removing a solvent-exposed side chain from water. Since their basis set consisted primarily of water soluble proteins with the normal distribution of solvent-exposed polar and apolar side chains, applying their value of ΔCp^o_{obs} to determine the number of side chains removed from water when dealing with a membrane-bound or membrane-associated protein should be done with caution. Nevertheless, using this average

value, the magnitude of the ΔCp^{o}_{obs} change upon mannitol binding to EII^{mtl}, corresponds to a removal of 50–60 amino acid side chains from contact with water. Clearly, significant conformational changes occur upon substrate binding.

One would like to have comparable data on P-EII^{mtl} but the substrate would dephosphorylate the enzyme. Titration of P-EII^{mtl} with perseitol is the best one can do to estimate the ΔCp^{o}_{obs} value of the P-B/C domain interaction. Although the K_d value did not change markedly upon phosphorylation of the enzyme, the values of ΔH^{o}_{obs} and ΔS^{o}_{obs} changed considerably. The decrease in ΔH^{o}_{obs} was compensated by a decrease in ΔS^{o}_{obs}, leaving the ΔG^{o}_{obs} value almost constant; another case of enthalpy–entropy compensation reflecting solvent rearrangement upon substrate binding. The associated ΔCp^{o}_{obs} value was less than 1 kJ K^{-1} mol^{-1}, considerably less than observed in the non-phosphorylated enzyme. This corresponds to less than six residues undergoing changes in their microenvironment. The large difference in the number of amino acids undergoing changes upon substrate binding in the non-phosphorylated versus phosphorylated enzyme could indicate that phosphorylation of the protein itself induces docking of the B domain on the C domain, and that docking is finished before substrate binding takes place. ITC experiments with vesicles treated with trypsin to remove the A and B domains and titrated with mannitol also yielded a low ΔCp^{o}_{obs} value of -0.5 ± 0.2 kJ K^{-1} mol^{-1} again corresponding to less than 6 amino acid side chains removed from water. This is considerably less than the 50–60 residues estimated for mannitol or perseitol binding to the intact enzyme. Since the A domain has no functional contact with the C domain, the difference between these values can be attributed to eliminating B/C domain interactions.

In summary, based on the ΔCp^{o}_{obs} values and the perfect entropy-enthalpy compensation found under the various experimental conditions, large conformational changes occur at the B/C interface upon phosphorylation or substrate binding. The large drop in ΔCp^{o}_{obs} after removal of the A and B domain proves that B domain residues are involved in this process and that this domain is docking on the C domain during phosphorylation or mannitol binding. A part of the CB domain polypeptide could also become more structured during these events. The DSC results indicating that, in the presence of mannitol, part of the B domain becomes unfolded only at high temperatures together with the C domain, support this view [46]. These observations are in agreement with kinetic studies showing that phosphorylation of the B domain increases 1000-fold the rate of mannitol translocation by the C domain [29,30] and with studies showing that variation of the side-chain structure at position 384 in the B domain affected the kinetics of mannitol binding by EII^{mtl} [53].

7. Spectroscopic investigations

There is no structural information on EIIs, except for hydropathy predictions and fusion data defining the organization of the transmembrane helices and the effects of mutations on certain functions, reviewed above. Fluorescence spectroscopy can provide both structural and dynamic data if fluorescent moieties are situated at specific positions in the molecule. EII^{mtl} contains four tryptophan residues all located in the C domain at positions 30, 42, 109 and 117. Single tryptophan mutants have been constructed by replacing three of the four tryptophans by phenylalanine. In addition, an EII^{mtl} mutant without tryptophan (trypless) and the single tryptophan mutants W320 and W384 were constructed, the last tryptophan being situated in the B domain. All these mutants exhibit high binding affinity towards mannitol and, with the exception of W384, phosphorylate mannitol [54]. Without special precautions, significant impurities absorbing and fluorescing in the tryptophan spectral region accumulated on EII^{mtl} during purification. These originated primarily from stabilizers present in detergents and plasticizers leaching from plastics and rubber upon exposure of these materials to detergent solutions. Procedures developed to avoid these impurities eliminated all background in the tryptophan spectral region and enabled lifetime and anisotropy decay measurements [55]. The emission intensity of the individual tryptophans varied considerably. W320 showed a 1.4 times higher intensity than all four tryptophans present in wild-type EII^{mtl}. At this moment we have no explanation for this high quantum yield. In contrast, the W384 is almost completely quenched, most likely by

the tyrosine or a carboxylate group in the active center of the B domain near the C384 phosphorylation site (see Section 9.3). The accessibility of the tryptophans, determined by KI quenching is in agreement with the transmembrane distribution proposed in Fig. 2B. W30, W42 and W320 have been predicted to be situated in transmembrane helices, while W109 and W117 are predicted to be situated in the first cytoplasmic loop, where a higher solvent accessibility is expected. The emission maximum (λ^{max}) indicated that W30 and W320 are situated in a strongly hydrophobic environment, while W42, W109 and W117 are in a more hydrophilic environment, caused by solvent and/or neighboring polar residues.

The high spectral purity of the EII^{mtl} samples made it possible to analyze, for the first time, the tryptophan fluorescence of an integral membrane protein by time-resolved fluorescence techniques and determine the lifetime distribution and the rotational behavior of the tryptophan side chains in the nanosecond (ns) timescale [56]. All single tryptophan mutants showed multiple lifetimes with up to four components between 0.1–5.9 ns and corresponding mean lifetimes $\langle\tau\rangle$ between 2.6 and 4.2 ns. The mean lifetime increased for W30 and W42 upon the addition of mannitol indicating that residues in the first putative transmembrane helix are involved in, or at least responsive to, the mannitol binding process. In this respect, it is of interest to note that this helix is the most highly conserved helix in EII^{mtl} from various bacteria [3]. All five tryptophan studied were strongly immobilized since the anisotropy decay was not only caused by rotation of the side chains ($\phi_{int} = 0.7–4.7$ ns), but also by a much slower rotation of the whole protein (ϕ_{prot}). Only in the case of W30 could this slow component be resolved to $\phi_{prot} = 30$ ns, a value which is too fast to account for the rotation of the whole enzyme–micelle complex but could represent segmental rotation of the whole C domain or a portion of it. Addition of mannitol did not induce significant changes in the tryptophans' mobility, however a significant drop in the angular displacement value (ψ) of W109 was measured upon phosphorylation of the protein. This is the first experimental evidence for a residue in the C domain responding to phosphorylation of the B domain. Similar studies on other site specific single tryptophan mutants should provide a more detailed picture of the mannitol binding region and the B/C domain interface.

8. IIA structural and mechanistic investigations

X-Ray diffraction and multi-dimensional heteronuclear magnetic resonance (NMR) spectroscopy have been employed in the 3D structure determinations of IIA^{glc} from *E. coli*, *Bacillus subtilis* and *Mycoplasma capricolum*, and IIA^{man}, IIA^{mtl}, and IIA^{ntr} from *E. coli*. Although all these proteins are phosphorylated by the same phosphoryl donor, P-HPr, their structures and their association properties are quite different.

8.1. The glucose–sucrose family

IIA^{glc} is by far the most thoroughly studied of the group. In *E. coli*, EII^{glc} consists of a $IICB^{glc}$ protein and a separate IIA^{glc} whereas, in *B. subtilis*, the domains are fused into a single polypeptide, $IICBA^{glc}$. The fused A domain has been subcloned and the structure compared with that of the *E. coli* enzyme. The proteins share 41% identical amino acids. *B. subtilis* IIA^{glc} is active in vivo and in vitro [57]. It can replace *E. coli* IIA^{glc} in glucose fermentation [58] and in regulating non-PTS sugar transport and metabolism [57,59]. Two electrophoretically distinct forms of *E. coli* IIA^{glc}, termed IIA^{glc}-fast and slow, have been isolated [60]. The 'slow' form is the mature protein; the 'fast' form is a proteolytic degradation product lacking the N-terminal 7 amino acids [61]. Although it could be phosphorylated by P-HPr, it had only 5% to 10% of the mature form's capacity to pass the phosphoryl group on to glucose suggesting that the missing peptide formed a portion of the recognition site for the B domain of $IICB^{glc}$. The conserved histidines, H75 and H90 in *E. coli* IIA^{glc} correspond to H68 and H83, respectively, in the *B. subtilis* protein. Phosphorylation of IIA^{glc} occurs on the $N^{\varepsilon 2}$ position of the histidine ring [60,62].

To determine the role of the histidines, Reizer et al. [63] replaced the *B. subtilis* H68 and H83 each with alanine and showed, in both cases, a loss of in vivo glucose transport activity and the various regulatory activities. Persper et al. [64] replaced the *E.*

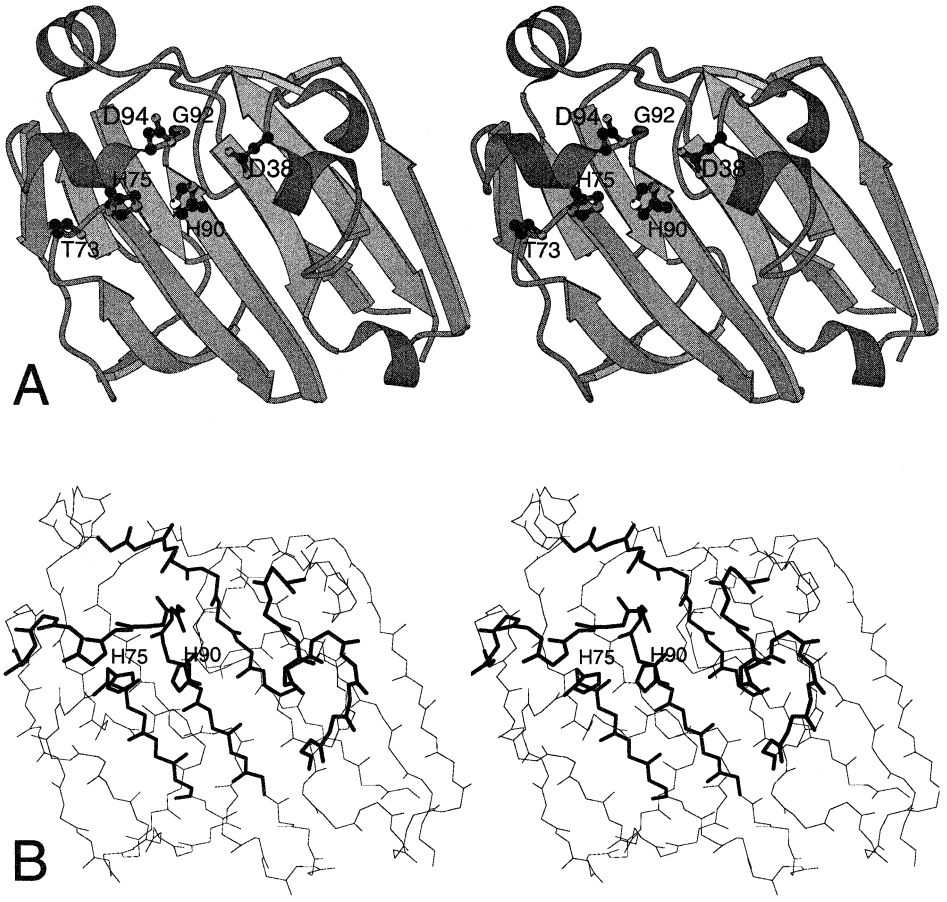

Fig. 5. Stereo representation of the structure of *E. coli* IIA^{glc}. PDB accession code 1F3G. (A) Backbone representation plus residues involved in the active site. The $N^{\delta 1}$ of H75 is pointing towards the side chain of residue 73 and the $N^{\delta 1}$ of H90 is pointing towards G92. The $N^{\varepsilon 2}$ nitrogen phosphorylation position is colored white. (B) The highlighted portions indicate residues for which changes in chemical shifts were observed upon phosphorylation of H90. They correspond to residues 36–46, 75–78, 87–110, and 131–138.

coli H90 and H75 by glutamines. Both mutants were inactive in in vitro glucose phosphorylation assays. While Q90–IIA^{glc} could not be labeled by ^{32}P-HPr, Q75–IIA^{glc} could still be labeled but was unable to transfer its phosphoryl group to glucose. These data confirmed H90 as the phosphoryl binding site but implicate H75 somehow in the phosphoryl group transfer to IIB^{glc}.

X-ray and multi-dimensional heteronuclear NMR have been employed to determine the crystal and solution structures of IIA^{glc} from *E. coli* [65–67] and *B. subtilis* [68–71]. In general, they reveal the molecule as an imperfect β-barrel or a β-sheet sandwich constructed of two sections of six antiparallel β-strands plus a few short distorted helices including 3_{10} helices (see Fig. 5A). Using the *E. coli* numbering, H90, the site of phosphorylation by P-HPr is situated at the C-terminus of β-strand 7 while H75, necessary for the phosphoryl donor activity to IIB^{glc} resides in a loop at the N-terminal end of strand 6, close enough to H90 to share a proton between the $N^{\varepsilon 2}$s of both histidine rings. This arrangement supports the suggestion made from mutagenesis studies that the two histidines could function in concert in phosphoryl transfer from P-HPr to IIB^{glc}. The active site which sits in a depression, is surrounded by a ring of hydrophobic residues on the surface which have been suggested to form the binding sites for P-HPr and IIB^{glc}. H90 $N^{\delta 1}$ is H-bonded to the backbone carbonyl oxygen of G92, while the H75 $N^{\varepsilon 2}$ is oriented towards the $O^{\gamma 1}$ of T 73, but too far away to be H-bonded (see Fig. 5A). The same arrangement is found in the *B. subtilis* protein. Liao et al. [68] also noted two Asp residues, D38 and D94, near the ac-

tive site, with approaching carboxylate moieties (4.7 Å) which they suggested could interact with positively charged residues during the interaction of IIA^{glc} with P-HPr or IIB^{glc}. Mutation of the Asp equivalent to D94 in the A domain of the homologous *E. coli* $IICBA^{bgl}$ to Ala reduced the catalytic activity of the enzyme, in keeping with a possible role for these residues, albeit indirect, in the catalytic process [72]. Three areas of the peptide chain were found to have a higher than average mobility in the *B. subtilis* structure as judged by ^{15}N-NMR relaxation measurements: the N-terminal 13 residues, residues 21–41 and residues 146–149 [73]. This may indicate participation of some of these residues in protein–protein interactions.

8.1.1. The mechanism of phosphoryl group transfer

After assigning backbone NMR resonances and identifying NOEs in *E coli* IIA^{glc}, the exercise was repeated for IIA^{glc} phosphorylated in situ with excess *P*-enolpyruvate, and catalytic amounts of EI and HPr [74]. The majority of chemical shifts were identical with those in the spectra of the unphosphorylated IIA^{glc}. However, changes were observed for peptide backbone NH, ^{15}N, $^{13}C\alpha$ and $H\alpha$ chemical shifts of residues V36–V46, H75–S78, L87–G100 and A131–V138, all of which are situated in the vicinity of the active site (see Fig. 5B). The largest chemical shift changes occur for residues in segment H90–L98 which forms a ridge close to the side chains of H90 and H75. These limited changes are most likely due to small structural rearrangements or differences in shielding as a consequence of phosphorylation. The fact that the NOE cross-peak patterns do not change upon phosphorylating the enzyme, even for residues which exhibit changes in chemical shifts, indicate that large conformational changes do not occur in the active site upon phosphorylation. However, pronounced changes in intensity were observed for the NOE cross peaks between the D94 NH and both T95 NHs and H90 CH^{ε}. Since the intensity of T95 and H90 NOEs to other residues did not change, the D94 NOE changes suggest that, upon phosphorylation, the NH of D94 moves towards the CH^{ε} of H90 and away from the NH of T95. This would be consistent with the NH of D94 H-bonding to a phosphoryl group oxygen. Deuterium exchange kinetics confirmed this interpretation. Both amide proton resonances disappear within 6 min after the addition of D_2O to IIA^{glc}; however, in P–IIA^{glc}, these amide proton resonances only disappeared 13 min after addition of D_2O. The fact that large structural rearrangements in IIA^{glc} do not occur upon phosphorylation is important because the phosphorylation has a significant effect on the protein's role as a regulator in several systems.

Bachovchin and Roberts [75] showed that the ^{15}N chemical shifts of the imidazole ring nitrogens could be correlated with their protonation state thereby enabling a direct determination of the tautomeric state of histidine rings. ^{1}H–^{15}N-HMQC NMR spectra give this information directly. The $N^{\delta1}$ tautomer of a neutral histidine is characterized by strong coupling of the $N^{\varepsilon2}$ to both $H^{\varepsilon1}$ and $H^{\delta2}$, giving two strong cross-peaks, while the $N^{\delta1}$ couples strongly only to $H^{\varepsilon1}$. Pelton et al. [76] used this approach to further characterize H90 and H75 in IIA^{glc} and P–IIA^{glc}. In both IIA^{glc} and P–IIA^{glc}, H75 occurs as the $N^{\varepsilon2}$ tautomer and H90 as the $N^{\delta1}$ tautomer with the phosphoryl group situated on $N^{\varepsilon2}$. The proton attached directly to the histidine ring nitrogens usually exchanges rapidly with solvent such that their NMR resonances cannot be observed, however, if they are buried or restrained in a H-bond, the resonances would be visible. The H90 $N^{\delta1}H^{\delta1}$ resonance could be observed in IIA^{glc} in keeping with a strong H-bond to the carbonyl oxygen of G92 but the H75 $N^{\delta1}H$ could not be observed even though, in both the *E. coli* and *B. subtilis* enzymes, it appears to be within H-bond distance of a $ThrO^{\gamma1}$. In P–IIA^{glc}, both the H90 $N^{\delta1}H$ and H75 $N^{\varepsilon2}H$ resonances were visible. Thus, the presence of the phosphoryl group attached to H90 decreases the exchange rate of the H75 $N^{\varepsilon2}H^{\varepsilon2}$. In IIA^{glc}, both histidines are neutral while in P–IIA^{glc}, H75 is neutral and H90 is protonated. The imidazole ring resonance positions for both IIA^{glc} and P–IIA^{glc} were essentially independent of pH between 6 to 9, indicating that the rings do not change their protonation state in this range.

An analysis of the *E. coli* IIA^{glc} mutants H75Q and H90Q has provided more insight into the H-bond geometry at the active site [77]. Neither mutation has significant effect on the structure of the protein beyond the direct vicinity of the active site, but there are alterations in thermodynamic stability

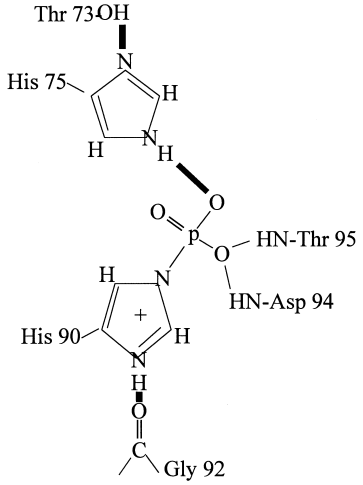

Fig. 6. The interaction of residues involved in the phosphoryl group transition state at the active site of IIA^{glc} as suggested by Pelton et al. [76]. The hydrogen bonds are indicated with thick black lines.

which reflect entropic and enthalpic changes due to altered H-bond geometries and mobilities of the residues in the active center. The Q90 $N^{\delta 1}$ still forms a H-bond to the same acceptor as H90 in the wild-type protein, but the Q75 H-bond geometry is altered and the mobility of the residue appears to be increased. The H-bonding and tautomeric states of the histidines were determined by ^{15}N–^{1}H-HMQC NMR spectra similar to the analysis presented above for the wild-type protein [76]. As with wild-type IIA^{glc}, the chemical shifts of the histidine resonances in both mutants were invariant with pH, both histidines being unprotonated in the non-phosphorylated protein while H90 was protonated in the phosphorylated protein. The chemical shift of the Q75 side chain amide nitrogen and one of its protons alter significantly upon phosphorylation of H90, consistent with it entering into a H-bond with the phosphoryl group. However, it does not appear to be H-bonded to the $T73O^{\gamma 1}$ as H75 is in the wild-type protein. A schematic for the proposed H-bond geometry at the active site of the wild-type phosphorylated protein is presented in Fig. 6. It shows the trigonal bipyramid transition state for the transfer of the phosphoryl group from P–IIA^{glc} as expected on the basis of the inversion of configuration observed by Begley et al. [78]. Pelton et al. suggest that the absence of the $T73O^{\gamma 1}$ H-bond may be the basis for the 200-fold lower rate of phosphoryl group transfer to IIB^{glc} in the H75Q mutant protein [77,79]. A 200-fold rate reduction corresponds to approximately 3 kcal/mol decrease in the free energy of activation for the transfer reactions and this is within the range expected for the loss of a H-bond. A probable mechanism accounting for the rate reduction is that the glutamine amide is much less acidic than the H75 $N^{\varepsilon 2}H$, especially when H75 is, in turn, H-bonded to $T73O^{\gamma 1}$. The less acidic glutamine amide is less capable of polarizing the P–O to which it is H-bonded, thus leaving a less electrophilic P which is less reactive with the incoming nucleophilic histidine of the phosphoryl group acceptor molecule. Since the H-bond is present in the absence of the phosphoryl group acceptor molecule, the effect of the H75Q mutation would be a ground-state stabilization of P–IIA^{glc}. More information could be obtained by looking directly at the effect of the mutation on the P–O moiety by ^{31}P-NMR or by vibrational spectroscopy. Such data is not yet available. That such subtle alterations in bond polarity can have dramatic effects on reaction rates is amply documented, for instance, with the serine esterases [80].

8.1.2. Interaction with other proteins

The phosphotransferase system, in *E. coli*, functions both in the transport of PTS carbohydrates and in the regulation of the transport of non-PTS carbohydrates [1]. IIA^{glc} plays a central role in both processes, in the case of PTS carbohydrates, via its interactions with P-HPr and $IICB^{glc}$ and, in the case of non-PTS carbohydrates, via its interactions with other proteins responsible for their transport or metabolism. To date, detailed information has been collected on the interaction of IIA^{glc} with HPr and glycerol kinase, the former with the *B. subtilis* enzyme and the later with the *E. coli* enzyme. HPr–IIA^{glc} interactions were defined with the help of ^{15}N-edited and ^{15}N-filtered NMR experiments using uniformly ^{15}N-labeled IIA^{glc} and unlabeled HPr, both from *B. subtilis* [81]. The largest amide proton and nitrogen chemical shift changes involve resonances from residues 31–40 which are part of the loop at the top of the molecule close to the phosphorylation site, and residues 61–64, 70–72, 79–81 and 132–134 in the β-strands which participate in the sheet holding the two essential histidines (see Fig. 5B). The regions of HPr showing the largest changes included

the phosphorylation site residue H15, 16–23 in the same helix and sections 43–47 and 51–56 comprising a loop and a section of β-sheet, respectively. Herzberg has modeled the HPr/IIA^{glc} complex by linking the active site histidines of the two proteins with a pentacoordinated phosphate which is presumed to occur in the phosphorylation transition state [82]. A salt bridge was identified in the computer-generated model between HPr R17 and the residue comparable to D38 which presumably plays a role in stabilizing the complex and/or orienting the active sites of the two proteins. Support for the importance of salt bridges in protein complexes with IIA^{glc} comes from the recent analysis of the crystal structure and packing of *M. capricolum* IIA^{glc} [83]. Two neighboring molecules associate with one another in the crystal in a front-to-back fashion such that a glutamic acid side chain of one molecule forms electrostatic interactions with the active site histidines of the other. A second salt bridge occurs between an aspartic acid side chain in the IIA^{glc} active site and a lysine of the neighboring molecule. When the HPr/IIA^{glc} and IIA^{glc}/IIB^{glc} complexes are modeled as done by earlier, ion pairs are found between two invariant aspartate residues of IIA^{glc} and an Arg or Lys residue of HPr or IIB^{glc}. The authors conclude that these are the main interactions which determine the specific orientations of the active sites of the phosphoryl donors and acceptors during the transfer process, while non-specific hydrophobic interactions provide a loose recognition element for the initial complex formation and account for the ability of IIA^{glc} to 'recognize' a variety of structurally distinct proteins.

E. coli IIA^{glc} is a non-competitive inhibitor of glycerol kinase [84] (GK) but its inhibition is eliminated by phosphorylation [85]. To understand the basis for the inhibition, the X-ray structure of IIA^{glc}-(slow) complexed with glycerol kinase in the presence of glycerol and ADP was determined [86]. Glycerol kinase exists both as a dimer and a tetramer in solution but, in the crystal, it is a tetramer with one IIA^{glc} bound to each monomer. The structure of IIA^{glc} does not change upon complexation. The major interaction between GK and IIA^{glc} buries 1300 Å^2 of surface area and involves the active site region of IIA^{glc}, including residues 38–46, 71,78, 88, 90 and 94–97, and GK residues 402 and 472–481 more than 30 Å removed from the GK active site (see Fig. 7). These residues comprise two turns of a 3_{10}-helix linked to a longer α-helix by a 45° bend. They fit into the concave active site of IIA^{glc}, the dominant interactions between the two proteins being hydrophobic. The hydrophobic ring around the IIA^{glc} active site interacts with the aliphatic portions of GK residues 472–479. There appears to be little similarity between the IIA^{glc} contact sites for GK and HPr except that each possesses an arginine two residues on the C-terminal side of the residue interacting with H90 in IIA^{glc}, (R17/H15 in HPr and R479/T477 in GK). In GK/IIA^{glc}, GK-R479 makes a salt bridge with IIA^{glc}-D38. This is analogous to the salt bridge discussed in the preceding paragraph. This is one of only two salt bridges made in the complex. The GK

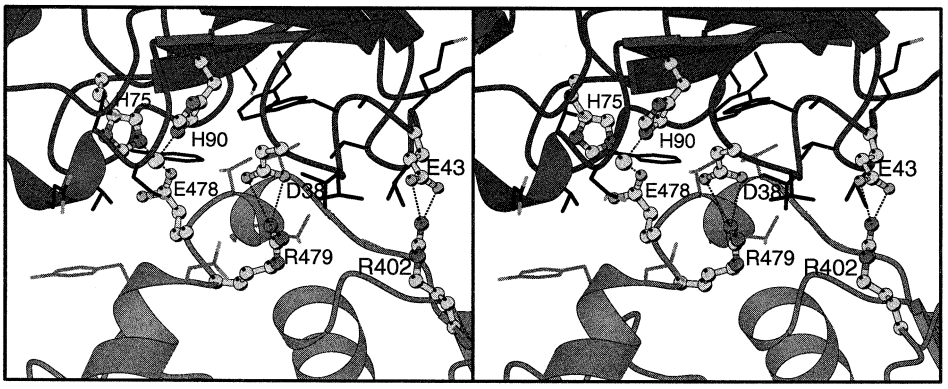

Fig. 7. Stereo representation of the interface of *E. coli* glycerol kinase:IIA^{glc} complex. The complex also contains glycerol-3-phosphate, adenosine diphosphate, Mg^{2+} and Zn^{2+}. PBD accession code 1glc. The salt bridges which stabilize the complex are D38:R479 and E43:R402. A zinc ion is coordinated between the IIA^{glc} active site residues H75 and H90 and E478 from glycerol kinase.

site is a more ordered helix while the HPr site N-terminal to H15 is a coil. It should be noted, however, that the GK–IIA^{glc} contact site is defined by an X-ray structure of the cocrystallized complex while inferences about the HPr–IIA^{glc} contact site are based on modeling data using the free HPr structure rather than a structure of cocrystallized HPr/IIA^{glc} complex. GK residues 472–481 are disordered in GK alone and only form a 3_{10}-helix in complex with IIA^{glc} [87]. A similar complexation-induced structural change could also be happening in the P-HPr–IIA^{glc} complex.

A zinc ion was found in the refined GK–IIA^{glc} X-ray structure at the interface between the two proteins. Its ligands were H75 and H90 from IIA^{glc} and E478 from GK. The glutamate side chain rotates relative to its position in the complex in the absence of zinc in order to form this site. In vitro inhibition of GK by IIA^{glc} in the absence of zinc could not explain the strong inhibition observed in vivo. Coordination of the zinc, however, results in a 15-fold decrease in the K_i and is consistent with the complete inhibition of GK in vivo by physiological concentrations of IIA^{glc}. Similar discrepancies reported between in vitro measurements and in vivo data for the regulation of LacY and MelB by IIA^{glc} [88–90] have led Feesre et al. [87] to suggest that 'cation-promoted association' may be a general feature of protein–protein interactions. It would allow strong complex formation using a minimal number of amino acid side chains and so enable a protein like IIA^{glc} to interact strongly with a variety of structurally different molecules. The reason that P–IIA^{glc} does not form a stable complex with GK appears to be threefold: (i) steric hindrance of the phosphoryl group in the GK binding site, (ii) a lack of positive charge in the GK binding site to stabilize the negatively charged phosphate and several other negatively charged groups which come together in the complex, and (iii) destruction of the zinc coordination site.

8.2. The mannose–sorbose family

The *E. coli* mannose transporter consists of three proteins, a soluble IIBA^{man} and two membrane-bound proteins, IIC^{man} and IID^{man} [13]. IIBA^{man}, in turn, consists of two domains linked by a flexible Ala-Pro-rich linker. The N-terminal A domain is phosphorylated from P-HPr, accepting the phosphoryl group on the N$^{\varepsilon 2}$ position of H10. The C-terminal B domain, is phosphorylated from the A domain, accepting the phosphoryl group on the N$^{\delta 1}$ position of H175 [16]. The function of the Ala-pro-rich linker in the activity and the dynamics of IIBA^{man} has been examined by altering the length of this segment at the gene level. Truncation and extension by 142 extra amino acids decreased but did not abolish the activity in vivo or in vitro whereas a 3-fold increase in length had no effect, suggesting that the length is not critical for the function unless it becomes too short. Phosphorylation studies with intact IIBA^{man} and phosphorylation site mutants as well as isolated domains have shown that phosphoryl group transfer between HPr, IIA and IIB is reversible and that transfer can occur between domains within one protein as well as between domains of different proteins.

The IIBA^{man} domains were separated by limited trypsinolysis after partial purification and the structure of the A domain structure has been investigated by heteronuclear NMR [91] and X-ray diffraction [92]. The protein forms a stable dimer with a mass of 31 kDa. Multidimensional heteronuclear NMR provided the first insight into the 3D structure, indicating that, in contrast with IIA^{glc}, it belongs to the α/β-fold class. The NMR showed that it consisted of a five-stranded β sheet with the strand order 2, 1, 3, 4, 5, with strands 2, 1, 3, 4 parallel and strand 5 antiparallel. Subsequently, strand 5 was seen from the X-ray structure to originate from the adjacent molecule in the dimer; it is presumably responsible for stabilizing the dimer. That the terminal helix and strand are not integral components of the A domain was confirmed with the observation of mannose PTS activity in vivo when a truncated IIA^{man} lacking these elements was coexpressed with plasmids coding for the IIB^{man}, IIC^{man} and IID^{man} proteins. The strands are connected by α-helices (see Fig. 8). H10 and S72, both essential for activity, are located in adjacent loops. H10 is situated in the loop connecting the first β-strand and α-helix and S72 is situated in the loop connecting the third β-strand and α-helix. Since heterodimers consisting of monomers each carrying a mutation in one of these residues were inactive, the two loops on one domain must form a functional active site. This is supported by additional

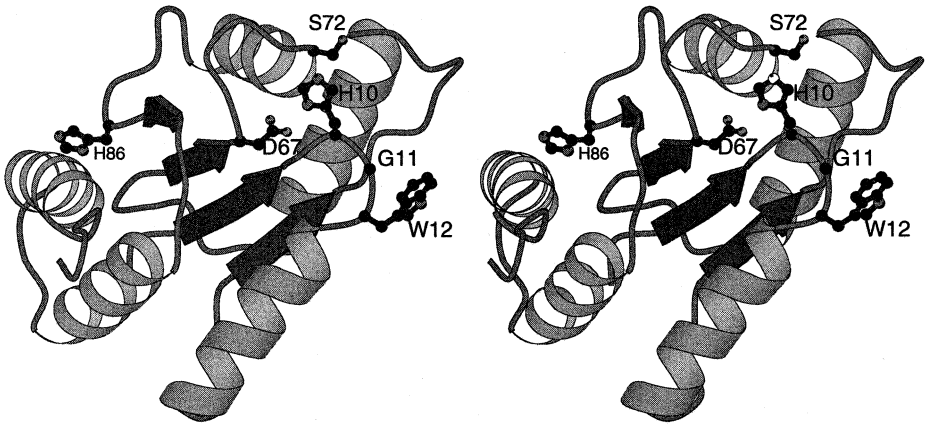

Fig. 8. Stereo representation of the X-ray crystallographic structure of *E. coli* IIA^{man} [92]. PDB accession code 1PDO. The fifth strand suggested by the NMR structure is not included because it originates from the adjacent molecule in the dimer.

mutagenesis data. The mutation W12F results in greater than 90% decrease in activity but its effects can be reversed by a second mutation at W69F such that the activity of the double mutant W12,69F is comparable to wild-type protein [93]. Sequence comparisons support a functional role for residues in these two loops as well. G11 in loop one and the sequence around S72 in loop three are highly conserved in the LevD and SorF subunits of the *B. subtilis* fructose transporter [94] and the *K. pneumoniae* sorbose transporter [95], proteins structurally related to IIA^{man}.

The notable differences in the active site arrangement between IIA^{man} and IIA^{glc} are (i) that the N-1 position of H10 is H-bonded to the carboxylate of a completely buried Asp 67, and (ii) that there is no other adjacent histidine in the active site. The H-bond to the Asp is reminiscent of the His–Asp pair in the serine esterases where it has been suggested that the Asp alters the nucleophilicity of the histidine during catalysis [96–98]. It is questionable whether the Asp fulfills the same function in IIA^{man} especially since, in IIA^{glc}, the comparable H-bond acceptor is a peptide carbonyl oxygen. The function of the H-bond acceptor could be simply to stabilize the position of the imidazole ring similar to that observed in HPr [99]. ^{1}H- and ^{15}N-NMR chemical shift information on the H10 imidazole ring nitrogens would be helpful in addressing this issue, but it is not yet available.

Mutagenesis studies reported that H86 was absolutely required for transfer of the phosphoryl group to IIB^{man}, but not necessary for the phosphorylation of IIA^{man} by P-HPr reminiscent of similar results with IIA^{glc}. This was surprising considering the location of H86 at the opposite side of the molecule from the active site. Resequencing of the vector used in this study indicated that a mix-up had occurred during subcloning and that the protein used was a His/Cys mutant of the B domain phosphorylation site, which explains the phenotype (B. Erni, personal communication).

8.3. The mannitol–fructose family

The *E. coli* mannitol-specific PTS consists of a IICBA^{mtl} protein. The domains have been subcloned [45,100–103] IIA^{mtl} consists of 48% α-helix and 23% β-sheet as judged by FTIR analysis [104] and HSQC NMR spectra [105]. This is in marked contrast to IIA^{glc}, but is more in line with IIA^{man}. IIA^{mtl} is homologous to IIA^{fru} and IIA^{ntr}, the latter being the product of ORF162, of the *rpoN* operon which is transcribed along with the rpoN gene coding σ^{54}; the σ-factor activates the transcription of genes for nitrogen assimilation [106]. These three proteins show sequence homology especially in the region of the conserved histidine. The structures of IIA^{mtl} and IIA^{ntr} have been solved very recently by X-ray crystallography [107,108]. They contain a novel fold consisting of a central β-sheet in which two pairs of parallel β-strands are oriented antiparallel to each other and flanked on one side by a fifth short strand (Fig. 9). The fold is also different from that of IIA^{glc}

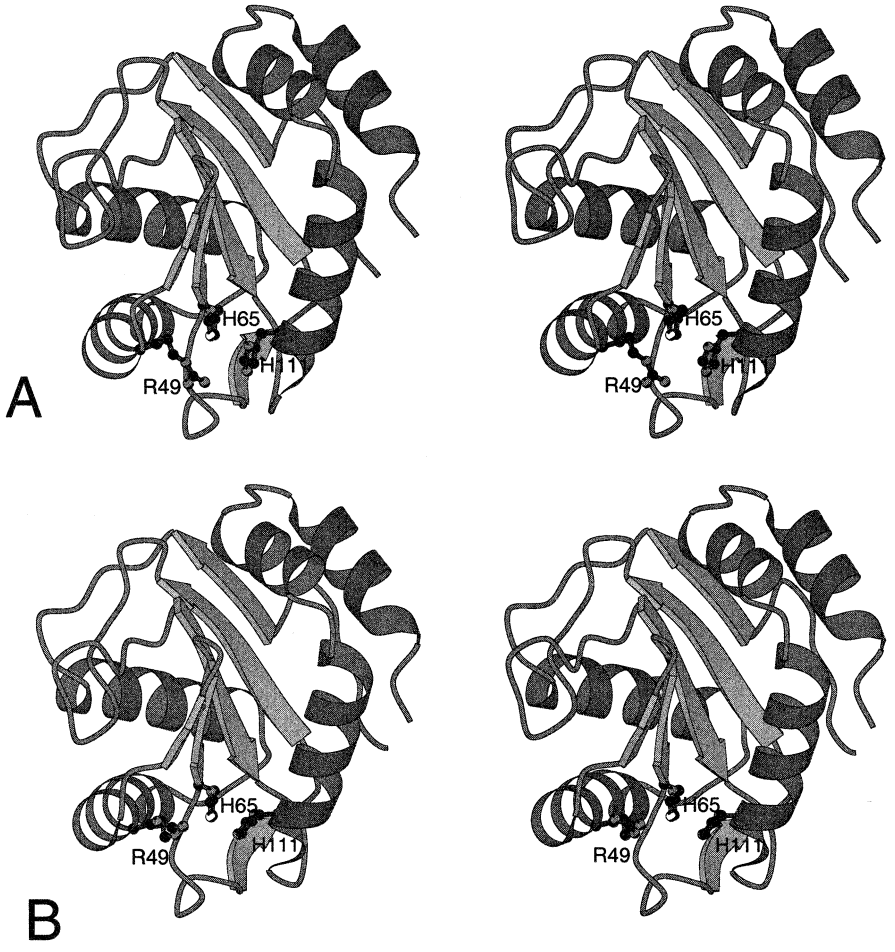

Fig. 9. Stereo representation of *E. coli* IIA^{mtl}. PDB accession code 1A3A with the active site H65 Nε2 atom colored white. Panels A and B show the two different arrangements of R49 and H111 seen in the two molecules in the dimer.

and IIA^{man}. Although the structures are homologous there are differences in the region of the active site which may bear on the different functions of the two proteins. In IIA^{mtl}, the active site histidine, H65, is situated in a shallow depression, mostly buried, and surrounded on the surface by a ring of hydrophobic residues similar to that observed in IIA^{glc}. The $N^{\delta 1}$ of H65 is H-bonded to a peptide carbonyl oxygen; this arrangement is also analogous to that seen in IIA^{glc}. It may function to stabilize the residue in its phosphorylated form or simply to fix the orientation of the phosphoryl group-accepting $N^{\varepsilon 2}$. This portion of the imidazole ring is slightly exposed to solvent. H65 is situated in between two residues, R49 and H111, which are strongly conserved in IIAs of the mannitol–fructose family and thought, therefore, also to be involved in the phosphoryl transfer process.

Van Dijk et al. [109] used ^{1}H–^{15}N-HSQC NMR spectra of selectively ^{15}N-histidine labeled protein to define the tautomeric and H-bonded states of the three histidines of IIA^{mtl} and P–IIA^{mtl}. The active site histidine has a pK_a of less than 5.8. The spectra indicate that, in the neutral form, the ring exists unmistakably as the $N^{\varepsilon 2}$ tautomer. Furthermore, neither ring nitrogen is H-bonded as evidenced by the ^{15}N resonance positions of 129 ppm and 209 ppm for $N^{\delta 1}$ and $N^{\varepsilon 2}$, respectively. The crystal structure, however, indicates the occurrence of a H-bond between the $N^{\delta 1}$ and a backbone carbonyl; therefore, we would expect the $N^{\delta 1}$ tautomer and a H-bond as in the case of *E. coli* IIA^{glc}. Upon phosphorylation, the NMR shows that the pK_a increases to 8.7 which should put the histidine into the protonated state at neutral pH with the $N^{\delta 1}$ now protonated and able to

form a H-bond. The ^{15}N chemical shifts, however, suggest that the ring is protonated but not H-bonded, but it could also be unprotonated and strongly H-bonded. The electron distribution can be strongly influenced by the presence of the phosphoryl group and H-bonding. It is probably safer to rely on the combined X-ray and NMR data which together would indicated a H-bonded system similar to that found in P–IIA^{glc}.

The discrepancy between the NMR and X-ray data is significant; we have no way of reconciling the two data sets at the present time except by invoking a real difference in the orientation of the H65 in the crystal versus solution. In this regard, it is worth noting that the phosphorylation site H189 in the N-terminal domain of the PTS *E. coli* EI undergoes a conformational change involving the χ_2 angle upon phosphorylation and upon protonation so that the $N^{\varepsilon 2}$ phosphoryl-accepting site which is solvent inaccessible in the non-phosphorylated protein can be phosphorylated [110]. A similar type of movement could explain the NMR data on IIA^{mtl} and P–IIA^{mtl}.

The second histidine at the active site, H111, corresponds to His C of van Dijk et al. [109]. Of the two other histidines in IIA^{mtl}, His B has pK_as of 7.3 and 7.46 in the unphosphorylated and phosphorylated state, respectively. This histidine, in both the unphosphorylated and phosphorylated protein, exists in a rapid tautomeric equilibrium in the neutral form. The pK_a of His C changes from 6.7 to 7.15 upon phosphorylation of H65, but it remains as the $N^{\delta 1}$ tautomer irrespective of the phosphorylation state, with the $N^{\delta 1}$ being moderately H-bonded in the unphosphorylated protein whereas neither ring N is H-bonded in the phosphorylated protein. The NMR data showed the occurrence of four sets of cross peaks in the HSQC spectra of both IIA^{mtl} and P–IIA^{mtl}, indicating that one of the three histidines must alternate between two conformations in slow exchange on the NMR time scale. While it could not be unambiguously assigned by NMR, the crystallographic data offer an explanation. Four IIA^{mtl} molecules, organized as two pairs of dimers, are found in the asymmetric unit of IIA^{mtl} crystals. Comparison of Fig. 9A and B show that the two molecules in the dimer differ in the arrangement of H111 and R49 at the active site. In one molecule, the R49 side chain points away from the active site, while H111 is oriented parallel to H65. In the other, the R49 side chain is situated close to the phosphorylation site, while H111 points away from H65 and does not interact with other residues. Van Montfort et al. [107] suggest that these two configurations might reflect the two active site geometries involved in the phosphoryl group accepting and donating states of the protein. Models were generated of a phosphoryl group transfer transition state complex between P-HPr and IIA^{mtl}, followed by energy minimization using the two different configurations. In one configuration, the R49 guanidium moiety forms two H-bonds with the phosphoryl oxygens of the trigonal bipyramid transition state whereas no H-bonds were seen between the transition state phosphoryl group and either R49 or H111 in the other configuration. As in the case of IIA^{glc}, we do not have enough data to define, unambiguously, the function of these residues. The two configurations could represent the state of these side chains before and after phosphorylation of IIA^{mtl} or they could represent states on the reaction path for the phosphorylation or dephosphorylation of IIA^{mtl}. P-NMR and vibrational spectroscopic data on the state of the phosphoryl group in the native enzyme as well as mutants lacking H111 and R49 are needed.

The most significant difference between IIA^{ntr} and IIA^{mtl}, from a mechanistic point of view, is the orientation of H120 in IIA^{ntr}. As discussed above, H111, its equivalent in IIA^{mtl}, is pointing into the active site region in both of the orientations found in the crystal structure whereas, in IIA^{ntr}, it is situated on the back side of a helix facing away from the active site and cannot be reoriented without a significant untwisting of the helix. At the present time, there is no evidence that IIA^{ntr} phosphorylates another protein. It could carry out its regulatory function by binding to some other component, in a manner similar to *E. coli* IIA^{glc}. In such a case, phosphoryl transfer in the 'forward' direction would not be required and the second histidine, which has been implicated in the 'forward' transfer would not be necessary.

8.4. The lactose–cellobiose family

Staphylococcus aureus IIA^{lac} occupies a special place in the family of PTS IIA members. It was first

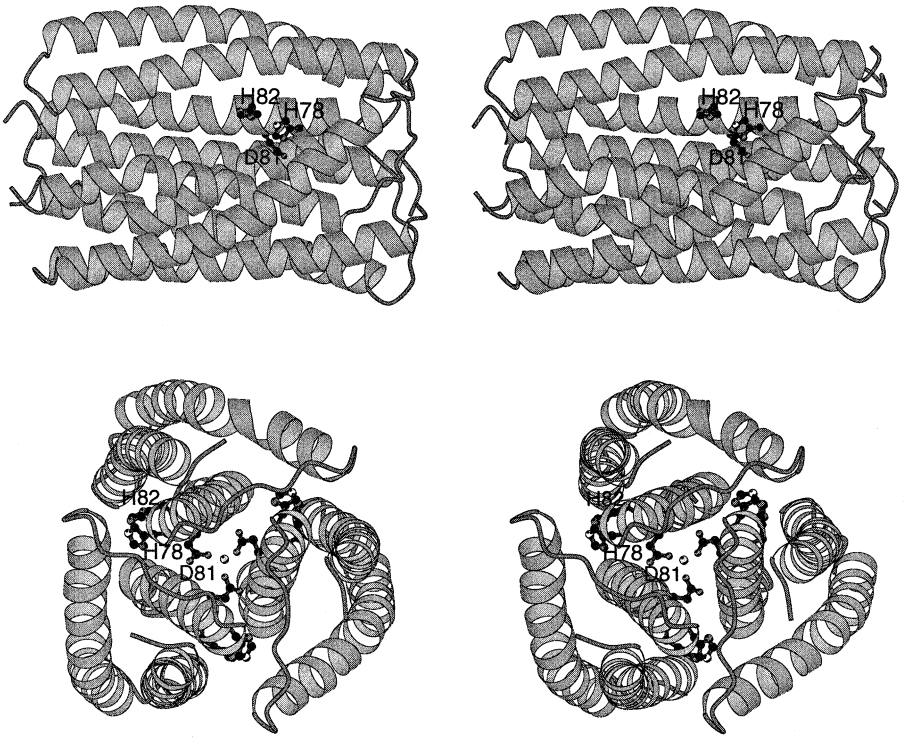

Fig. 10. Stereo representation of the structure of *L. lactis* IIA^{lac}. PDB accession code 1E2A. Top panel is the view from the side of the trimer with one phosphorylation site clearly visible. The Nε2 phosphorylation position on H78 is indicated in white. The other residues shown are D81 and H82. Bottom panel is the view from the end of the trimer along the superhelical axis with the D81 metal binding residue from each monomer pointing into the center of the coiled-coil.

isolated as a 33 kDa protein [111] and shown to be a trimer whose association state could be destabilized upon phosphorylation [112]. ^{1}H-NMR has shown that one of the four histidines in the monomer, H19, becomes phosphorylated at the N$^{\varepsilon 2}$ position and that the pK_a of this histidine changes upon phosphorylation from 6.0 to 8.6 [113]. The chemical shifts of many of the ^{1}H-NMR resonances in IIA^{lac} change significantly with temperature between 30°C and 60°C, indicating that the protein interconverts between two states rapidly on the NMR time-scale. Significant conformational changes upon phosphorylation were reflected in a decrease in helix content from 42% to 25%, as judged by CD, and an inability of antibodies raised against IIA^{lac} to precipitate P–IIA^{lac} [114]. At least part of these changes was assigned to the peptide carrying the phosphoryl group on the basis of an anomalous pH titration behavior of tyrosine resonances in the phosphorylated versus non-phosphorylated peptide. Finally when a mixture of IIA^{lac} and P–IIA^{lac} were run on a Sephadex-100 column in the presence of Triton X-100, IIA^{lac} migrated at the same position in the presence as in the absence of Triton X-100 whereas P–IIA^{lac} migrated considerably faster in the presence of Triton X-100 as though it had associated with the detergent micelles. Taken in their entirety, the results are consistent with a conformational change upon phosphorylation which causes the trimer to dissociate to monomers and interact with a hydrophobic surface [114]. The N-terminus of IIA^{lac} is thought to be responsible for this interaction since an isolated N-terminal 38 residues peptide effectively inhibited phosphoryl group transfer from P–IIA^{lac} to IICB^{lac}. This is analogous to the result seen with IIA^{glc} 'fast' which lacked the N-terminal 7 residues of the mature protein and was incapable of transferring its phosphoryl group to IICB^{glc}. However, a similar relationship between phosphorylation state, association state and membrane interaction has yet to be documented for another IIA protein.

The crystallographic structure confirms the extra-

ordinary difference between IIA^{lac} and members of other IIA families. *Lactococcus lactis* IIA^{lac} crystallizes as a trimer, each monomer consisting of a single peptide chain with 3 α-helical segments which fold to form a triple α-helical bundle. Together, the monomers form a coiled-coil superhelical structure with helix 3 from each monomer forming the interface (see Fig. 10) [115]. The superhelix is stabilized by a single metal at the center of the bundle that coordinates to the same D81 from all three monomers and by hydrophobic interactions between the these helices. This segment also provides the active site residues, H78, the phosphorylation site, and H82. The relative orientation of these two residues is very similar to that found in IIA^{glc} and, again, implicates two histidines in the mechanism of phosphoryl group transfer. Phosphorylation of the three active sites at the interfaces of the monomers in the superhelical bundle may be one of the driving forces for the conformational changes seen upon phosphorylation; these, in turn, may be reporting the dissociation of the complex into its individual subunits before binding to the membrane [114].

9. IIB structural and mechanistic studies

9.1. The glucose–sucrose family

IIB^{glc} from *E. coli* was obtained by subcloning from the gene encoding the wild-type transporter with covalently-linked B and C domains [45]. The ^{15}N or $^{15}N/^{13}C$-enriched protein was produced for resonance assignments and 3D structure determination by multi-dimensional heteronuclear NMR techniques [116–118]. The backbone assignments and NOE contacts indicate that the overall fold is a split α/β sandwich with the secondary structure order α1β1β2α2β3β4α3. The active site cysteine, residue 35 (C421 in $IICB^{glc}$), is situated at the C-terminal end of the first β-strand, preceding a loop. It and a series of conserved hydrophilic residues are exposed to the solvent on one face of the β-sheet (Fig. 11) surrounded by a larger patch of hydrophobic residues. It is likely that the hydrophobic patch directs the initial binding recognition to IIA^{glc}, as has been suggested for HPr/IIA complexes, while the hydrophilic residues are responsible for fine-tuning the geometry of the complex and assisting in the mechanism of phosphoryl group transfer. The exposed nature of the cysteine is in keeping with the observations from HPr/IIA complexes that geometries of the PTS donor acceptor complexes are complementary. The active site of IIA is retracted into a shallow depression while that of both proteins which must interact with it, HPr and IIB^{glc}, protrude into solution. The chemical shift changes upon formation of a IIA^{glc}/IIB^{glc} complex involve only resonances of residues in and surrounding the two active site regions; no major conformational changes result from binding.

Phosphorylation [118] effects mainly the region

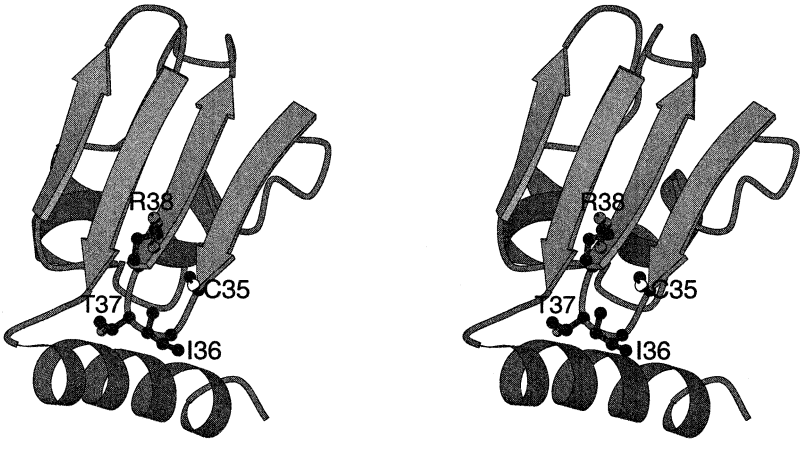

Fig. 11. Stereo representation of *E. coli* IIB^{glc} PDB accession code 1IBA. The active site residue C35 is colored black. Residues I36, T37 and R38 are those for which the intensity of the cross-peaks for the amide backbone increases upon phosphorylation, suggesting a reduction in flexibility.

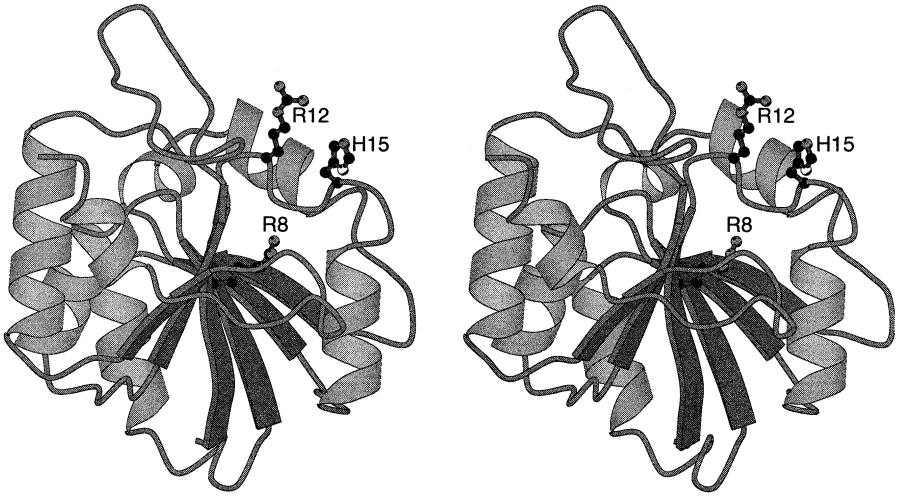

Fig. 12. Stereo representation of the X-ray structure of *B. subtilis* IIB^{lev}. PDB accession code 1BLE. R8 and R12 are conserved residues essential for phosphorylation activity. The Nδ1 atom of the phosphorylation site histidine in marked in white.

around the active site cysteine, residues 32–40, as expected if the cysteine protrudes into solution. These effects are reflected in changes in the chemical shifts of amide backbone resonances, as well as changes in ^{1}H–^{1}H-NOESY cross-peak positions and in the intensity of ^{15}N-HSQC cross-peaks. The later indicates that backbone dynamics are altered; spectra of the unphosphorylated protein show only low intensity cross-peaks for the amide backbone protons of residues I36, T37 and R38 most likely due to exchange broadening as this region of the protein adopts different conformations. Upon phosphorylation, the intensities increase suggesting a tightening of the structure in this region possibly due to H-bonding between the phosphoryl group and neighboring side-chains.

9.2. The mannose–sorbose family

The NMR backbone assignments and secondary structure determination of the subcloned *E. coli* IIB^{man} and the *B. subtilis* IIB^{lev} have been reported [119,120] as well as an X-ray structure of *B. subtilis* IIB^{lev} [121]. The two proteins belong to the same family; their sequences are 47% identical and they possess histidine rather than a cysteine as the phosphorylation site residue. Both proteins adopt a fold not yet seen in other PTS proteins but found in nucleotide binding proteins, a six-stranded parallel β-sheet with a strand order, 3–2–4–1–5–6. The structure is a strongly twisted β-pleated sheet with helices 1 and 2 on one side and helices 3, 4 and 5 on the opposite side of the β-sheet. The active site histidine, H15, is readily accessible to solution. It is situated in the first loop, β1/α1, which is the topological switch point of the structure (Fig. 12). It is preceded by two conserved arginines which are essential for the phosphoryl transfer activity [120]. The loop carrying the H15 is exposed. The crystallographic β factors as well as the electron density in IIB^{lev} suggest that it is quite flexible. Weak NMR signal intensities for the first half of the β-sheet in IIB^{man} suggest that this portion of the molecule also experiences considerable conformational flexibility. The flexibilities are expected to play a role in stabilizing the bound phosphoryl group and allowing the conformational adaptability which is essential for interactions of IIB with its IIA and IIC/IID partners.

A parallel has been drawn between the global active site structures of HPr and IIB^{lev} or IIB^{man} because all three proteins interact with the same IIA^{man} and reversibly transfer their phosphoryl groups to this protein. Both in HPr and in these IIB species, the active site histidine is situated on a loop protruding into solution, able to penetrate into the shallow depression which forms the active site of IIA. Each is situated at the N-terminus of a helix whose helix dipole should assist in stabilizing the phosphorylated histidine. This dipole has been suggested to be the origin of the exceptionally low pK_a of the HPr active

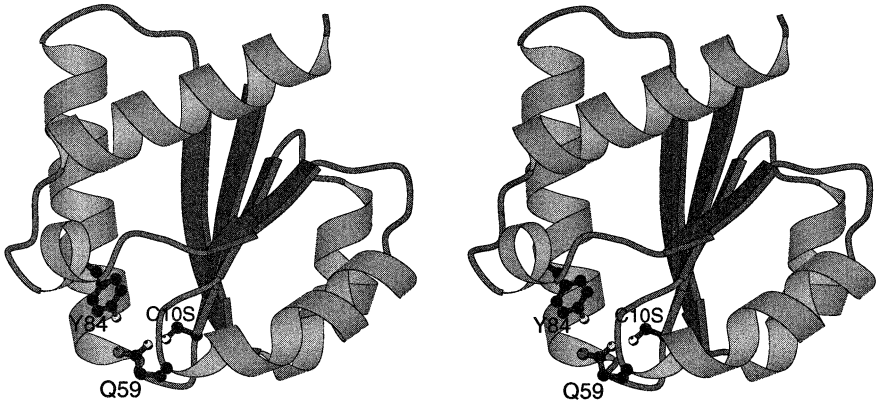

Fig. 13. Stereo representation of the X-ray structure of the *E. coli* C10S–IIB^{cel}. PDB accession code 1IIB. The phosphorylation site, position 10 plus Y84 and Q59 which may be involved in the phosphorylation activity are shown in ball and stick mode.

site histidine. It would be interesting to know whether this feature also carries over to the histidine in IIB. In HPr, the phosphoryl group on H15 is stabilized by H-bonds to backbone amides of residues 16 and 17 [122]. In IIB^{lev}, the position of H15 is such that H bonds between the phosphoryl group and the backbone amides of residues 16 and 17 are also possible. Since it was experimentally shown that IIA^{man} could replace IIA^{lev} in the phosphoryl transfer from HPr, it was deemed trustworthy to model the IIA^{man}/IIB^{man} complex using the crystal structure coordinates of IIA^{man} and IIB^{lev}. The same procedure was followed as in the previous modeling of HPr/IIA complexes, linking the active site histidines by a pentacoordinated phosphoryl group and rotating about this axis to search for favorable interaction geometries. As in the case of the glucose systems analyzed by Herzberg and coworkers [83], a favorable geometry was found in which the complex would be stabilized by a salt-bridge between an active site Arg from the B domain and an Asp from the A domain.

9.3. The lactose–cellobiose family

The *E. coli* cellobiose-specific EII^{cel} consists of three separate components IIC^{cel}, IIB^{cel} and IIA^{cel} [123,124]. The structure of IIB^{cel} has been determined by both X-ray diffraction and NMR. The X-ray structure, with a resolution of 1.8 Å, shows that the protein is an α/β structure consisting of a central four-stranded parallel twisted β-sheet with the strand order 2, 1, 3, 4, surrounded by α-helices (Fig. 13). The active site cysteine is situated at position 10 at the end of the first β-strand, preceding the loop (P loop) which connects this strand to the following helix [125,126]. The NMR structure determination has resulted in an identical structure [127,128] with differences mainly in the clarity of the loop regions. The NMR data provide insufficient restraints for residues in the loops, resulting in apparent disorder. This may be real and may be due to conformational averaging. The loop is most likely involved in stabilizing the phosphoryl group bound to C10 in P–IIB^{cel}, as is the macro-dipole from the following helix which points with its N-terminus towards this loop. A structure of the phosphorylated species will be necessary before this can be stated with certainty. The 3D structure is most similar to that of bovine liver low molecular mass phosphotyrosine phosphatase (PTPase) [129], also a protein constructed from an α/β fold with the same strand order and with its catalytic cysteine at the C-terminal end of the first β-strand. The same folding motif is found at the core of the whole family of PTPases, some of which are considerably larger than the bovine enzyme [130]. The catalytic cysteine, in the PTPases, is followed by a loop with a signature sequence, C–X–X–X–X–X–R. The X-ray structure of the protein containing tungstate at the active site as a phosphate analogue, shows backbone atoms of the loop residues and the guanidium moiety of the conserved Arg form H-bonds to the tungstate group and may stabilize the phosphate moiety in the phosphorylated protein [131]. Eberstadt et al. [117] find the same general signature sequence in IIB^{glc} and suggest that the ar-

Fig. 14. Stereo representation of the *E. coli* arabinose binding protein complexed with D-galactose [139]. PBD accession code 8ABP. The galactose and K10 are shown in the ball and stick mode.

ginine may not only be involved in stabilizing the phosphoryl group in the phosphorylated enzyme, but may also play a role in activating the cysteine by shifting it towards the thiolate form. This suggestion follows from the PTPase studies where the pK_a of the active site cysteine is 4.67 [132]. However, there is no clear evidence that the B domain cysteine has such a low pK_a. The pK_a of NEM inactivation in *R. sphaeroides* EII^{frc} was approximately 7.8 [133]; since phosphorylation protected against inactivation, we can conclude that the pK_a of 7.8 belongs to the active site residue in this protein. In the case of EII^{mtl}, Boer et al. [53] reported that the pH dependence of the mannitol exchange kinetics of the C domain were determined by the presence of the B domain and the nature of the residue at the position of the active site C384. In the absence of the B domain, there was no pH dependence in the pH range 6–9, whereas with the native B domain attached, the exchange kinetics showed a pK_a of 7.5–8 while the mutant proteins, C384S and C384E, had pK_as in the range of 7.0–7.5. Thus, it is likely that the pK_a of the active site cysteine in the B domain is not abnormally low, at least, not in the resting protein. If arginine is playing a role in polarizing the cysteine on the way to the transition state, some other residue must be responsible in IIB^{cel} and IIB^{mtl} since these proteins lack an arginine in the loop sequence and the 3D structure of IIB^{cel} shows no arginine anywhere near the active site. There is, however, a tyrosine H-bonded to the cysteine sulfhydryl moiety in IIB^{cel} (Fig. 13) and it is conserved in *E. coli* IIB^{mtl}. In IIB^{mtl}, it is the only tyrosine and Meijberg et al. [134] observed that its fluorescence was red-shifted at pH values higher than pH 6 indicative of the tyrosinate state. This arrangement has been found in the active site of glutathione-*S*-transferase where the role of the tyrosine has been suggested to be one of providing electrophilic stabilization of the thiolate anion by donating a hydrogen bond (TyrOH...$^-$SE) in the ground and transition state for nucleophilic addition [135] or, acting as a tyrosinate anion general base (TyrO$^-$...HSE), to abstract the proton from the sulfhydryl group [136]. Whether the IIB tyrosine is present as a tyrosinate and whether either of these roles can be attributed to the tyrosine in IIB^{cel} and IIB^{mtl} will require further study.

A structure alignment search of the PDB revealed strong structural homology of IIB^{cel} not only to PTPase, but also to the N-terminal domain of the

arabinose binding protein (ABP). It too is an α/β structure composed of a four-stranded parallel β-sheet (Fig. 14). Near the position of the conserved tyrosine in IIB^{cel}, we find a phenylalanine in ABP. Aromatic residues are known to be involved in carbohydrate binding [137] and indeed, in the structure of ABP with D-galactose bound, the galactose is in contact with the phenylalanine. It is possible that the tyrosine in IIB^{cel} forms part of the cellobiose binding site. In this regard, it is enticing to note that a lysine in ABP is found at residue 10 and that it occupies the same position as the active site cysteine in IIB^{cel}. In the complex with D-galactose bound, the lysine εNH_2 is positioned within H-bond contact with a hydroxyl of carbohydrate. The ABP-carbohydrate complex might serve as the paradigm for the last step in cellobiose transport, where it is bound at the cytoplasmic site just prior to phosphorylation by the B domain and release into the cytoplasm.

10. IIC structural studies

Studies dealing with the mechanism of the transmembrane movement and phosphorylation of carbohydrate have been discussed earlier as have the disposition of the C domain in the membrane (see Sections 1, 4 and 6). Very little is known about the structure of any of the C domains of PTS EIIs. FTIR studies on the IIC^{mtl} domain indicate that the protein consists of 42% α-helix, 26% β-sheet and the remainder as random coil (unpublished data). The low content of α-helix is consistent with the hydropathy analysis and fusion data of Jacobson and coworkers (see Fig. 2B) which predict that approximately 50% of the amino acids in the C domain do not fold into transmembrane α-helices [12]. Even though mannitol has a significant effect on the C domain as judged by DSC measurements, its presence causes no alteration of the FTIR spectra suggesting that mannitol binding to the C domain alone does not grossly alter the folding of the protein.

Brisson and coworkers have succeeded in crystallizing the C domain of *E. coli* EII^{mtl} in two dimensions and have obtained crystals of high enough order to provide a clear 5Å projection map of the protein by cryo-electron crystallography [138]. The protein crystallizes as a dimer with the dimer interface centered around a two-fold axis. Electron density attributable to the individual transmembrane helices is clearly visible. They offer hope of soon understanding the relative positions of the transmembrane helices and the overall folding on the non-helical portions of the peptide chain.

11. Conclusion

The ensemble of mechanistic studies being done on members of the PTS EII family, together with detailed three-dimensional data which is becoming available on both the water-soluble and membrane-bound transporter domains, promises to provide a detailed molecular description of the events surrounding phosphate-energy-coupled solute transport within the next several years.

References

[1] P.W. Postma, J.W. Lengeler, G.R. Jacobson, Microbiol. Rev. 57 (1993) 543–594.
[2] J.S. Lolkema, G.T. Robillard, New Compr. Biochem. 21 (1992) 135–167.
[3] J.W. Lengeler, K. Jahreis, U.F. Wehmeier, Biochim. Biophys. Acta 1188 (1994) 1–28.
[4] B. Erni, Int. Rev. Cytol. 137 (1992) 127–148.
[5] M. Meins, P. Jeno, D. Muller, W.J. Richter, J.P. Rosenbusch, B. Erni, J. Biol. Chem. 268 (1993) 11604–11609.
[6] G.J. Ruijter, G. van Meurs, M.A. Verwey, P.W. Postma, K. van Dam, J. Bacteriol. 174 (1992) 2843–2850.
[7] B. Erni, Biochemistry 25 (1986) 305–312.
[8] A. Buhr, B. Erni, J. Biol. Chem. 268 (1993) 11599–11603.
[9] J.W. Lengeler, F. Titgemeyer, A.P. Vogler, B.M. Wohrl, Phil. Trans. R. Soc. Lond. B Biol. Sci. 326 (1990) 489–504.
[10] J.S. Lolkema, H. Kuiper, R.H. ten Hoeve Duurkens, G.T. Robillard, Biochemistry 32 (1993) 1396–1400.
[11] H. Boer, R.H. ten Hoeve Duurkens, G.K. Schuurman Wolters, A. Dijkstra, G.T. Robillard, J. Biol. Chem. 269 (1994) 17863–17871.
[12] J.E. Sugiyama, S. Mahmoodian, G.R. Jacobson, Proc. Natl. Acad. Sci. USA 88 (1991) 9603–9607.
[13] B. Erni, B. Zanolari, P. Graff, H.P. Kocher, J. Biol. Chem. 264 (1989) 18733–18741.
[14] Q. Mao, T. Schunk, K. Flukiger, B. Erni, J. Biol. Chem. 270 (1995) 5258–5265.
[15] E. Rhiel, K. Flukiger, C. Wehrli, B. Erni, Biol. Chem. Hoppe Seyler 375 (1994) 551–559.
[16] B. Erni, B. Zanolari, H.P. Kocher, J. Biol. Chem. 262 (1987) 5238–5247.

[17] F. Huber, B. Erni, Eur. J. Biochem. 239 (1996) 810–817.
[18] Q. Mao, T. Schunk, B. Gerber, B. Erni, J. Biol. Chem. 270 (1995) 18295–18300.
[19] R. Lanz, B. Erni, J. Biol. Chem. 273 (1998) 12239–12243.
[20] A.P. Vogler, C.P. Broekhuizen, A. Schuitema, J.W. Lengeler, P.W. Postma, Mol. Microbiol. 2 (1988) 719–726.
[21] A.P. Vogler, J.W. Lengeler, Mol. Gen. Genet. 213 (1988) 175–178.
[22] M.M. Stephan, S.S. Khandekar, G.R. Jacobson, Biochemistry 28 (1989) 7941–7946.
[23] R.P. van Weeghel, Y.Y. van der Hoek, H.H. Pas, M. Elferink, W. Keck, G.T. Robillard, Biochemistry 30 (1991) 1768–1773.
[24] Q.P. Weng, J. Elder, G.R. Jacobson, J. Biol. Chem. 267 (1992) 19529–19535.
[25] H. Boer, R.H. ten Hoeve Duurkens, G.T. Robillard, Biochemistry 35 (1996) 12901–12908.
[26] Q.P. Weng, G.R. Jacobson, Biochemistry 32 (1993) 11211–11216.
[27] C.A. Saraceni Richards, G.R. Jacobson, J. Bacteriol. 179 (1997) 1135–1142.
[28] A. Buhr, G.A. Daniels, B. Erni, J. Biol. Chem. 267 (1992) 3847–3851.
[29] M.G. Elferink, A.J. Driessen, G.T. Robillard, J. Bacteriol. 172 (1990) 7119–7125.
[30] J.S. Lolkema, R.H. ten Hoeve Duurkens, D. Swaving-Dijkstra, G.T. Robillard, Biochemistry 30 (1991) 6716–6721.
[31] R. Manayan, G. Tenn, H.B. Yee, J.D. Desai, M. Yamada, M.H. Saier, J. Bacteriol. 170 (1988) 1290–1296.
[32] J.S. Lolkema, D. Swaving-Dijkstra, G.T. Robillard, Biochemistry 31 (1992) 5514–5521.
[33] W. Meijberg, G.K. Schuurman Wolters, G.T. Robillard, J. Biol. Chem. 273 (1998) 7949–7956.
[34] S.S. Khandekar, G.R. Jacobson, J. Cell. Biochem. 39 (1989) 207–216.
[35] J.S. Lolkema, R.H. ten Hoeve Duurkens, G.T. Robillard, J. Biol. Chem. 268 (1993) 17844–17849.
[36] J. Broos, R.H. ten Hoeve Duurkens, G.T. Robillard, J. Biol. Chem. 273 (1998) 3865–3870.
[37] M. Zulauf, in: H. Michel (Ed.), Crystallization of Membrane Proteins, CRC Press, Boca Raton, 1991, pp. 53–72.
[38] M. Corti, V. Degiorgio, J. Phys. Chem. 85 (1981) 1442–1445.
[39] J.S. Lolkema, G.T. Robillard, Biochemistry 29 (1990) 10120–10125.
[40] M.M. Stephan, G.R. Jacobson, Biochemistry 25 (1986) 4046–4051.
[41] P.G. Nilsson, B. Lindman, J. Phys. Chem. 87 (1983) 4756–4761.
[42] G. Komaromy-Hiller, N. Calkins, R. von Wandruszka, Langmuir 12 (1996) 916–920.
[43] A. Buhr, K. Flukiger, B. Erni, J. Biol. Chem. 269 (1994) 23437–23443.
[44] G.T. Robillard, H. Boer, R.P. van Weeghel, G. Wolters, A. Dijkstra, Biochemistry 32 (1993) 9553–9562.
[45] W. Meijberg, G.K. Schuurman-Wolters, G.T. Robillard, Biochemistry 35 (1996) 2759–2766.
[46] W. Meijberg, G.K. Schuurman-Wolters, H. Boer, R.M. Scheek, G.T. Robillard, J. Biol. Chem. 273 (1998) 20785–20794.
[47] Z. Markovic Housley, A. Cooper, A. Lustig, K. Flukiger, B. Stolz, B. Erni, Biochemistry 33 (1994) 10977–10984.
[48] R.N. McElhaney, Biochim. Biophys. Acta 864 (1986) 361–421.
[49] R.S. Spolar, M.T. Record, Science 263 (1998) 777–784.
[50] L.N. Lin, J. Li, J.F. Brandts, R.M. Weis, Biochemistry 33 (1994) 6564–6570.
[51] K. Takahashi, J.L. Casey, J.M. Sturtevant, Biochemistry 20 (1981) 4693–4697.
[52] J.S. Lolkema, E.S. Wartna, G.T. Robillard, Biochemistry 32 (1993) 5848–5854.
[53] H. Boer, R.H. ten Hoeve Duurkens, J.S. Lolkema, G.T. Robillard, Biochemistry 34 (1995) 3239–3247.
[54] D. Swaving-Dijkstra, J. Broos, J.S. Lolkema, H. Enequist, W. Minke, G.T. Robillard, Biochemistry 35 (1996) 6628–6634.
[55] D. Swaving-Dijkstra, J. Broos, G.T. Robillard, Anal. Biochem. 240 (1996) 142–147.
[56] D. Swaving-Dijkstra, J. Broos, A.J. Visser, A. van Hoek, G.T. Robillard, Biochemistry 36 (1997) 4860–4866.
[57] J.S. Reizer, S.L. Sutrina, L.-F. Wu, J. Deutscher, P. Reddy, M.H. Saier Jr., J. Biol. Chem. 267 (1992) 9158–9169.
[58] G. Gonzy-Treboul, M. Steinmetz, J. Bacteriol. 169 (1987) 2287–2290.
[59] D.A. Dean, J. Reizer, H. Nikaido, M.H. Saier Jr., J. Biol. Chem. 265 (1990) 21005–21010.
[60] N.D. Meadow, S. Roseman, J. Biol. Chem. 257 (1982) 14526–14537.
[61] N.D. Meadow, P. Coyle, A. Komoryia, C.B. Anfinsen, S. Roseman, J. Biol. Chem. 261 (1986) 13504–13509.
[62] M. Dorschug, R. Frank, H.R. Kalbitzer, W. Hengstenberg, J. Deutscher, Eur. J. Biochem. 144 (1984) 113–119.
[63] J. Reizer, S.L. Sutrina, L.-F. Wu, J. Deutscher, P. Reddy, M.H. Saier Jr., J. Biol. Chem. 267 (1992) 9158–9169.
[64] K.A. Persper, C.Y. Wong, L. Liu, D.W. Meadow, S. Roseman, Proc. Natl. Acad. Sci. USA 86 (1988) 4052–4055.
[65] D. Worthylake, N.D. Meadow, S. Roseman, D.-I. Liao, O. Herzberg, S.J. Remington, Proc. Natl. Acad. Sci. USA 88 (1991) 10382–10386.
[66] J.G. Pelton, D.A. Torchia, N.D. Meadow, C.-Y. Wong, S. Roseman, Proc. Natl. Acad. Sci. USA 88 (1991) 3479–3483.
[67] J.G. Pelton, D.A. Torchia, N.D. Meadow, C.-Y. Wong, S. Roseman, Biochemistry 30 (1991) 10043–10057.
[68] D.-I. Liao, G. Kapadia, P. Reddy, M.H. Saier Jr., J. Reizer, O. Herzberg, Biochemistry 30 (1991) 9583–9594.
[69] W.J. Fairbrother, J. Cavanagh, H.J. Dyson, A.G. Palmer, S.L. Sutrina, J. Reizer, M.H. Saier Jr., P.E. Wright, Biochemistry 30 (1991) 6896–6907.
[70] W.J. Fairbrother, G.P. Gippert, J. Reizer, M.H. Saier Jr., P.E. Wright, FEBS Lett. 296 (1992) 148–152.
[71] W.J. Fairbrother, A.G. Palmer III, M. Rance, J. Reizer, M.H. Saier Jr., P.E. Wright, Biochemistry 31 (1992) 4413–4425.

[72] K.S. Schnetz, S.L. Sutrina, M.H. Saier Jr., B. Rak, J. Biol. Chem. 265 (1990) 13464–13471.
[73] M.J. Stone, W.J. Fairbrother, A.G. Palmer III, J. Reizer, M.H. Saire Jr., P.E. Wright, Biochemistry 31 (1992) 4394–4406.
[74] J.D. Pelton, D.A. Torschia, N.D. Meadow, S. Roseman, Biochemistry 31 (1992) 5215–5224.
[75] W.W. Bachovchin, J.D. Roberts, J. Am. Chem. Soc. 100 (1978) 8041–8047.
[76] J.G. Pelton, D.A. Torchia, N.D. Meadow, S. Roseman, Protein Sci. 2 (1993) 543–558.
[77] J.G. Pelton, D.A. Torchia, S.J. Remington, K.P. Murphy, N.D. Meadow, S. Roseman, J. Biol. Chem. 271 (1996) 33446–33446.
[78] G.S. Begley, D.E. Hansen, G.R. Jacobson, J.R. Knowles, Biochemistry 21 (1982) 5552–5556.
[79] N.D. Meadow, S. Roseman, J. Biol. Chem. 271 (1996) 33440–33445.
[80] P.J. Tonge, P. Carey, Biochemistry 31 (1992) 9122–9125.
[81] Y. Chen, J. Reizer, M.H. Saier Jr., W.J. Fairbrother, P.E. Wright, Biochemistry 32 (1993) 32–37.
[82] O. Herzberg, J. Biol. Chem. 267 (1992) 24819–24823.
[83] K. Huang, G. Kapadia, P.-P. Zhu, A. Peterkofsky, O. Herzberg, Structure 6 (1998) 697–710.
[84] M.J. Novotny, W.L. Frederickson, E.B. Waygood, M.H. Saier Jr., J. Bacteriol. 162 (1985) 810–816.
[85] P.W. Postma, W. Epstein, R.J. Schuitema, S.O. Nelson, J. Bacteriol. 158 (1984) 351–353.
[86] J.H. Hurley, D. Worthylake, H.R. Faber, N.D. Meadow, S. Roseman, D.W. Pettigrew, S.J. Remington, Science 259 (1993) 673–677.
[87] M. Feesre, D.W. Pettigrew, N.D. Meadow, S. Roseman, S.J. Remington, Proc. Natl. Acad. Sci. USA 91 (1994) 3544–3548.
[88] M. Kuroda, S. de Waard, K. Mizushima, M. Tsuda, P. Postma, T. Tsuchiya, J. Biol. Chem. 267 (1992) 18336–18341.
[89] T. Misko, W. Mitchell, N. Meadow, S. Roseman, J. Biol. Chem. 262 (1987) 16261–16266.
[90] S. Dills, M. Schmidt, M.H. Saier Jr., J. Cell Biol. 18 (1982) 239–244.
[91] S. Seip, J. Balbach, S. Behrens, H. Kessler, K. Flukiger, R. de Meyer, B. Erni, Biochemistry 33 (1994) 7174–7183.
[92] R.S. Nunn, Z. Markovic-Housley, J.-C. Genovesio-Taverne, K. Flukiger, P.J. Rizkallah, J.N. Jansonius, T. Schirmer, B. Erni, J. Mol. Biol. 259 (1996) 502–511.
[93] Z. Markovic-Housley, J. Balbach, B. Stolz, J.-C. Genovesio-Taverne, FEBS Lett. 340 (1994) 202–206.
[94] I. Martin-Verstraete, M. Debarbouille, A. Klier, G. Rapoport, J. Mol. Biol. 214 (1990) 657–671.
[95] B.M. Wohrl, J.W. Lengeler, Mol. Microbiol. 4 (1990) 1557–1565.
[96] D.M. Blow, J.J. Birktoft, B.S. Hartley, Nature 211 (1969) 337–340.
[97] G.T. Robillard, R.G. Shulman, J. Mol. Biol. 71 (1972) 507–511.
[98] P.A. Frey, S.A. Whitt, J.B. Tobin, Science 264 (1994) 1927–1930.
[99] N.A.J. Van Nuland, R. Boelens, R.M. Scheek, G.T. Robillard, J. Mol. Biol. 246 (1995) 180–193.
[100] R.P. Van Weeghel, G. Meyer, H.H. Pas, W. Keck, G.T. Robillard, Biochemistry 30 (1991) 9478–9485.
[101] R.P. Van Weeghel, G.H. Meyer, W. Keck, G.T. Robillard, Biochemistry 30 (1991) 1774–1779.
[102] P.L. Grisafi, A. Scholle, J. Sugiyama, C. Briggs, G.R. Jacobson, J.W. Lengeler, J. Bacteriol. 171 (1989) 2719–2727.
[103] D.W. White, G.R. Jacobson, J. Bacteriol. 172 (1990) 1509–1515.
[104] P.I. Harris, G.T. Robillard, A.A. van Dijk, D. Chapman, Biochemistry 31 (1992) 6279–6284.
[105] G.J.A. Kroon, J. Grotzinger, K. Dijkstra, R.M. Scheek, G.T. Robillard, Protein Sci. 2 (1993) 1331–1341.
[106] B. Magasanik, Annu. Rev. Genet. 16 (1982) 135–138.
[107] R.L.M. Van Montfort, T. Pijning, K.H. Kalk, I. Hangyi, M.I.C.E. Kouwijzer, G.T. Robillard, B.W. Dijkstra, Structure 6 (1998) 377–388.
[108] D. Bordo, R.L.M. van Montfort, T. Pijning, K.H. Kalk, J. Reijzer, M.H. Saier Jr., B.W. Dijkstra, J. Mol. Biol. 279 (1998) 245–255.
[109] A.A. Van Dijk, R.M. Scheek, K. Dijkstra, G.K. Wolters, G.T. Robillard, Biochemistry 31 (1992) 9063–9072.
[110] D.S. Garrett, Y.-J. Seok, A. Peterkofsky, G.M. Clore, A.M. Gronenborn, Protein Sci. 7 (1998) 789–793.
[111] J.B. Hays, R.D. Simoni, S. Roseman, J. Biol. Chem. 248 (1973) 941–956.
[112] W. Hengstenberg, Curr. Top. Microbiol. Immunol. 77 (1977) 97–126.
[113] H.R. Kalbitzer, J. Deutscher, W. Hengstenberg, P. Rosch, Biochemistry 20 (1981) 6178–6185.
[114] J. Deutscher, K. Beyreuther, H.M. Sobek, K. Stuber, W. Hengstenberg, Biochemistry 21 (1982) 4867–4873.
[115] P. Sliz, R. Engelmann, W. Hengstenberg, E.F. Pai, Structure 5 (1997) 775–788.
[116] S. Golic Grdadolnik, M. Eberstadt, G. Gemmecker, H. Kessler, A. Burh, B. Erni, Eur. J. Biochem. 219 (1994) 945–952.
[117] M. Eberstadt, S. Golic Grdadolnik, G. Gemmecker, H. Kessler, A. Buhr, B. Erni, Biochemistry 35 (1996) 11286–11292.
[118] G. Gemmecker, M. Eberstadt, A. Buhr, R. Lanz, S. Golic Grdadolnik, H. Kessler, B. Erni, Biochemistry 36 (1997) 7408–7417.
[119] S. Seip, R. Lanz, R. Gutknecht, K. Flukiger, B. Erni, Eur. J. Biochem. 243 (1977) 306–314.
[120] R.M. Gschwind, G. Gemmecker, M. Leutner, H. Kessler, R. Gutknecht, R. Lanz, K. Flukiger, B. Erni, FEBS Lett. 404 (1997) 45–50.
[121] S. Schauder, R.S. Nunn, R. Lanz, B. Erni, T. Schirmer, J. Mol. Biol. 2 (1998) 591–602.
[122] N.A.J. Van Nuland, R. Boelens, R.M. Scheek, G.T. Robillard, J. Mol. Biol. 246 (1995) 180–193.

[123] H. Parker, B.G. Hall, Genetics 124 (1990) 455–471.
[124] J. Reizer, A. Reizer, M.H. Saier Jr., Res. Microbiol. 141 (1990) 1061–1067.
[125] R.L.M. Van Montfort, T. Pijning, K.H. Kalk, G.K. Schuurman-Wolters, J. Reizer, M.H. Saier Jr., G. Robillard, B.W. Dijkstra, J. Mol. Biol. 239 (1994) 588–590.
[126] R.L.M. Van Montfort, T. Pijning, K.H. Kalk, J. Reizer, M.H. Saier Jr., M.M.G.M. Thunnnissen, G.T. Robillard, B.W. Dijkstra, Structure 5 (1997) 217–225.
[127] E. AB, G.K. Schuurman-Wolters, J. Reizer, M.H. Saier Jr., K. Dijkstra, R.M. Scheek, G.T. Robillard, Protein Sci. 6 (1997) 304–314.
[128] E. AB, G.K. Schuurman-Wolters, M.H. Saier Jr., J. Reizer, M. Jacuinod, P. Roepstorff, K. Dijkstra, R.M. Scheek, G.T. Robillard, Protein Sci. 3 (1994) 282–290.
[129] X.D. Su, N. Taddei, M. Stefani, G. Ramponi, P. Nordlung, Nature 370 (1994) 575–578.
[130] D. Bradford, Curr. Opin. Struct. Biol. 5 (1995) 728–734.
[131] J.A. Stuckey, H.L. Schubert, E.B. Fauman, Z.-Y. Zhang, J.E. Dixon, M.A. Saper, Nature 370 (1994) 571–575.
[132] Z.-Y. Zhang, J.E. Dixon, Biochemistry 32 (1993) 9340–9345.
[133] J.S. Lolkema, R.H. Ten-Hoeve-Duurkens, G.T. Robillard, Eur. J. Biochem. 154 (1986) 651–656.
[134] W. Meijberg, G.K. Schuurman-Wolters, G.T. Robillard, Biochemistry 35 (1996) 2759–2766.
[135] S. Liu, P. Zhang, X. Ji, W.W. Johnson, G.L. Gilliland, R.N. Armstrong, J. Biol. Chem. 267 (1992) 4296–4299.
[136] W.M. Atkins, R.W. Wang, A.W. Bird, D.J. Newton, A.Y.H. Lu, J. Biol. Chem. 267 (1993) 4296–4299.
[137] C.L. Lawson, R. van Montfort, B. Strokopytov, H.J. Rozenboom, K.H. Kalk, G.E. de Vries, D. Penninga, L. Dijkhuizen, B.W. Dijkstra, J. Mol. Biol. 236 (1994) 590–600.
[138] R. Koning, G.K. Schuurnam-Wolters, G.T. Robillard, A. Brisson, Biophys. J. 74 (1998) A123.
[139] P.S. Vermersch, D.D. Lemon, J.J. Tesmer, F.A. Quiocho, Biochemistry 30 (1991) 6861–6866.